iScience

CellPress
OPEN ACCESS

Article

PRG-1 prevents neonatal stimuli-induced persistent hyperalgesia and memory dysfunction via NSF/Glu/GluR2 signaling

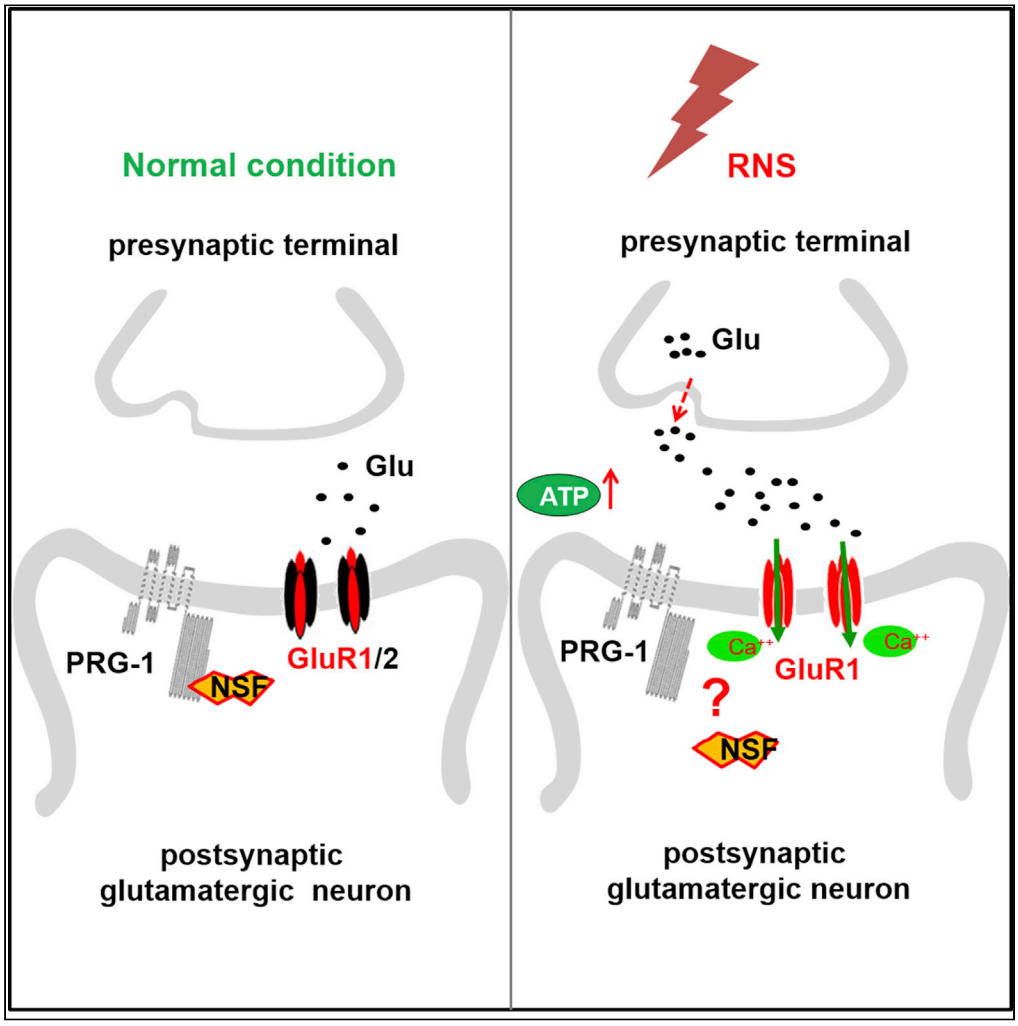

Xingfeng Liu, Site Li, Wenyu Zhang, ..., Song Cao, Tian Yu, Zhi Xiao

zyyutian@126.com (T.Y.)
zhixiao@zmu.edu.cn (Z.X.)

Highlights

Neonatal RNS induced hyperalgesia, learning, and memory impairment until adulthood.

PRG-1 attenuated RNS-induced impairments by dendritic spine regulation.

PRG-1 prevents RNS-induced impairments via NSF/Glu/GluR2 signaling.

Liu et al., iScience 25, 104989
September 16, 2022
https://doi.org/10.1016/j.isci.2022.104989

iScience

CellPress
OPEN ACCESS

Article

PRG-1 prevents neonatal stimuli-induced persistent hyperalgesia and memory dysfunction via NSF/Glu/GluR2 signaling

Xingfeng Liu,[1,2] Site Li,[3] Wenyu Zhang,[3] Zhuo Xie,[3] Jingxin He,[3] Xuanwei Zhang,[4] Shouyang Yu,[1,2] Song Cao,[5] Tian Yu,[1,2,6,*] and Zhi Xiao[1,2,6,7,*]

SUMMARY

Neonatal repetitive noxious stimuli (RNS) has been shown to cause long-term harmful effects on nociceptive processing, learning, and memory which persist until adulthood. Plasticity-related gene 1 (PRG-1) regulates synaptic plasticity and functional reorganization in the brain during neuronal development. In this study, neonatal RNS rats were established by repetitive needle pricks to neonatal rats on all four feet to model repetitive pain exposure in infants. Neonatal RNS caused thermal hyperalgesia, mechanical allodynia, learning, and memory impairments which manifested in young rats and persisted until adulthood. Hippocampal PRG-1/N-ethylmaleimide sensitive fusion protein (NSF) interaction was determined to be responsible for the RNS-induced impairment via enhanced extracellular glutamate release and AMPAR GluR2 trafficking deficiency in a cell-autonomous manner. These pathways likely act synergistically to cause changes in dendritic spine density. Our findings suggest that PRG-1 prevents the RNS-induced hyperalgesia, learning, and memory impairment by regulating synaptic plasticity via NSF/Glu/GluR2 signaling.

INTRODUCTION

Neonatal infants, especially preterm, are frequently subjected to painful repetitive procedures due to medical necessity (e.g., plantar blood collection, arteriovenous puncture, and tube insertions) in the neonatal intensive care unit (NICU) for many days after birth (Carbajal et al., 2008). Studies have suggested that pain perception and stress response may be more acute in premature than in full-term infants (Cannavo et al., 2022). Indeed, altered basal nociception leading to increased pain sensitivity in later life has been observed in subjects who had undergone NICU or neonatal surgery as infants (Hohmeister et al., 2010; Peters et al., 2005; Slater et al., 2010). Consequently, neonatal repetitive noxious stimulation (RNS) is now thought to cause long-term effects on nociceptive processing, learning, and memory which persist until adulthood (Knaepen et al., 2013).

Newborn infants display strong nociceptive behavior in response to repetitive painful and stressful exposures, and this is accompanied by neuronal activity generated in subcortical and cortical areas (Baxter et al., 2021; Verriotis et al., 2016). Neonatal RNS is associated with potentially adverse changes in central nervous system (CNS) development in both animal models (Schwaller and Fitzgerald, 2014) and human infants (Ranger and Grunau, 2014). One previous study showed that RNS was associated with greater noxious evoked activity in the brain, which could contribute to long-term activity-dependent plasticity in the adult CNS (Jones et al., 2017).

Plasticity-related genes (PRGs), also called lipid phosphate phosphatase-related proteins (LPPRs), are expressed specifically in vertebrate brain tissues and differentially regulated during brain development (Brauer et al., 2003; Strauss and Brauer, 2013). PRG-1/LPPR4, the first PRG family member to be characterized, has been shown to become expressed in the subventricular zone and hippocampal anlage as early as embryonic day 19 (E19) in rat (Brauer et al., 2003). After birth, PRG-1 expression increases dramatically in neocortex, hippocampus, and cerebellum until postnatal day 30 (P30), remains steady during maturation, then gradually drops to a low stable level in adulthood (Brauer et al., 2003).

[1]Guizhou Key Laboratory of Brain Science, Zunyi Medical University, Xuefu West Road 6, Xinpu District, Zunyi 563000, China

[2]Guizhou Key Laboratory of Anesthesia and Organ Protection, Zunyi Medical University, Xuefu West Road 6, Xinpu District, Zunyi 563000, China

[3]Graduate School, Zunyi Medical University, Zunyi 563000, China

[4]Clinical School, Zunyi Medical University, Zunyi 563000, China

[5]Department of Pain Medicine, Affiliated Hospital of Zunyi Medical University, Zunyi 563000, China

[6]Co-senior author

[7]Lead contact

*Correspondence: zyyutian@126.com (T.Y.), zhixiao@zmu.edu.cn (Z.X.)

https://doi.org/10.1016/j.isci.2022.104989

PRG-1 is expressed locally at the postsynaptic density of excitatory synapses on cortical and hippocampal glutamatergic neurons in adult brains of rats (Tokumitsu et al., 2010) and mice (Trimbuch et al., 2009). It plays an important role in maintaining synaptic homeostasis by controlling glutamatergic synapses (Trimbuch et al., 2009) and intracellular protein phosphatase 2A (PP2A)/β1-Integrin signaling (Liu et al., 2016). Deletion of PRG-1 causes increased lysophosphatidic acid (LPA) levels in the synaptic cleft and a higher presynaptic glutamate release probability. These neurochemical derangements ultimately lead to cortical network and hippocampal hyperexcitability, manifesting as epileptic seizures in mice (Trimbuch et al., 2009). One study reported that intracellular PRG-1/PP2A/β1-Integrin signaling could affect hippocampal spine numbers in CA1 stratum radiatum (sr) and CA1 stratum oriens (so), as well as molecular layer of dentate gyri (moDG) regions and memory formation (Liu et al., 2016). However, whether PRG-1 also plays a role in RNS-induced pain and neurodevelopment is completely unknown.

To address these questions, we established a rat model to evaluate the impact of repetitive neonatal pain stimuli on pain perception, learning, and memory in later life. Our findings suggest that hippocampal PRG-1 is involved in the regulation of RNS-induced pain hypersensitivity, learning, and memory deficiency which persist until adulthood in rats. Based on the results of this study, a scientific discovery of the interaction of PRG-1/N-ethylmaleimide sensitive fusion protein (NSF) has been revealed for modulating RNS-induced pain. Specifically, we found that PRG-1/NSF regulates dendritic spine development in hippocampus via extracellular Glu secretion and switching from GluR2-containing Ca^{2+} impermeable AMPARs to GluR2-lacking Ca^{2+} permeable AMPARs in a cell-autonomous fashion. Collectively, these findings suggest that PRG-1 prevents RNS-induced impairments in rats by regulating synaptic plasticity via NSF/Glu/GluR2 signaling pathway.

RESULTS

Evaluation of body weight and sensorimotor function after RNS or pharmacological intervention

In order to evaluate the impact of RNS during the neonatal period, we measured weekly changes in body weight and motor function in rats after RNS procedure or drug injections. No effect of RNS on body weight was observed for any observation time points from birth (week 0) to adulthood (week 9) (Figure 1A, $p > 0.05$).

To determine whether RNS, viral, or drug treatment affected proprioception and motor function, the inclined plane test was used. No effect of RNS procedure or any concomitant treatment on these parameters was observed (Figure 1B).

Impact of RNS on algesia

Behavioral responses to noxious stimuli are generally used as a model of pain perception in animal models and human infants (Mogil, 2009). To determine response to neonatal RNS in our model, we measured thermal withdrawal latency (TWL) and mechanical withdrawal threshold (MWT) every two weeks in the rats from 1 week until 9 weeks of age (Figures 1C and 1D). Interestingly, TWL time in control (CON) rats remained relatively stable from infancy to adulthood, while MWT pressure increased gradually in CON rats and stabilized in adulthood. These findings are in line with what has previously been reported (Hoogen et al., 2020; Knaepen et al., 2013). Conversely, neonatal RNS caused significant decreases in TWL and MWT values progressively from week 1 through week 9 (1-way ANOVA, $p < 0.05$ compared with CON group at the same observation time point, Figures 1C and 1D), suggesting that neonatal RNS causes development of thermal hyperalgesia and mechanical allodynia in rats.

Altered spatial learning and memory following neonatal RNS

A Morris Water Maze test (MWM) was used to determine whether neonatal RNS altered the development of spatial learning and memory. In the MWM test, RNS rats spent significantly longer time and traveled greater distances to arrive at the target in all three stages of life development up to adults (weeks 3, 6, and 9) compared with age-matched CON group (1-way ANOVA, $p < 0.001$; Figures 1E–1J). Moreover, RNS rats spent significantly less time in the quadrant zone that previously contained the platform than CON rats at week 6 and 9 (1-way ANOVA, $p < 0.001$; Figure 1K) but not at week 3, as determined by probe trials. We also assessed the mean speed in MWM test, which showed that RNS procedure, virus, and drug injections did not impair motor function of rats (Figure 1L). Overall, the above results suggested that RNS rats displayed clear spatial learning and memory deficits, rather than a putative impaired motor function.

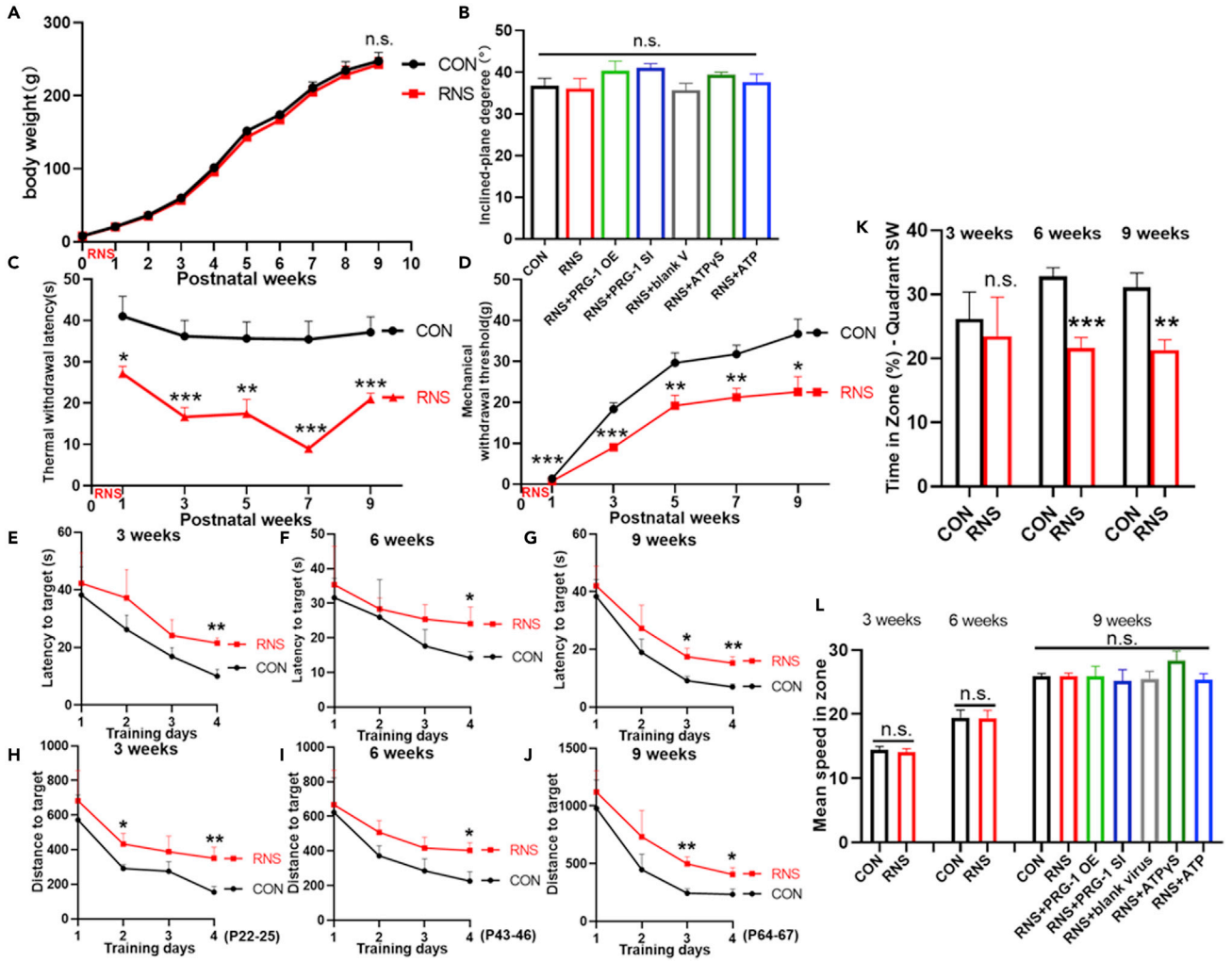

Figure 1. Pain, learning, and memory impairments in rats following neonatal RNS

(A) RNS procedure in neonatal rats didn't induce a change in body weight throughout the duration of the experiment from birth to adulthood (0–9 weeks). (Two-tailed unpaired student t test, $p > 0.05$).

(B) Inclined plane test indicated that experimental procedures, such as neonatal RNS, hippocampal viral infection, or drugs microinjection didn't impair motor function in the rats (n = 6; one-way ANOVA with Bonferroni post hoc, $p > 0.05$ among all groups).

(C and D) The TWL (C) and MWT (D) on the hind limb, which were measured after RNS procedure at weeks 1, 3, 5, 7, and 9 after birth, were significantly decreased in RNS rats compared with age-matched controls (n = 6; two-tailed unpaired student t-test, *: vs CON group at the same time point).

(E–K) Rats were trained to find the hidden platform under the water surface in spatial acquisition trials (E–J) and then tested in a probe trial without the platform 24 h after the last training trial (K).

(E–G) RNS rats show prolonged escape latency time to target on the fourth day compared with CON group on week 3, 6, and 9.

(H–J) RNS rats show longer escape path length to target compared with CON group on the fourth day at weeks 3, 6, and 9.

(K) Probe trials show that RNS rats spent significantly less time in the quadrant zone that previously contained the platform as compared with CON rats at week 6 and 9 but not week 3 (n = 6; two-tailed unpaired student t-test, *: vs CON group at the same time point).

(L) Mean speed in MWM test shows that RNS procedure, microinjections of virus, or drugs didn't impair motor function of rats (n = 6; two-tailed unpaired student t-test at 3 and 6 weeks, one-way ANOVA with Bonferroni post hoc at 9 weeks; $p > 0.05$ among all groups).

Data are presented as mean ± SEM with n.s. $p > 0.05$, *$p < 0.05$, **$p < 0.01$, ***$p < 0.001$; RNS, repetitive noxious stimuli; TWL, thermal withdrawal latency; MWT, mechanical withdrawal threshold; OE, overexpression; SI, silencing.

Hippocampal PRG-1 is involved in RNS-induced pain

Hippocampal expression of PRG-1 was high in CON group at 3 weeks of age and further increased by 6 weeks, then decreased to a low level by 9 weeks (adulthood) as shown by Western blot (Figures 2A and 2B), in line with previous report (Brauer et al., 2003). Compared to the CON group at same timepoints,

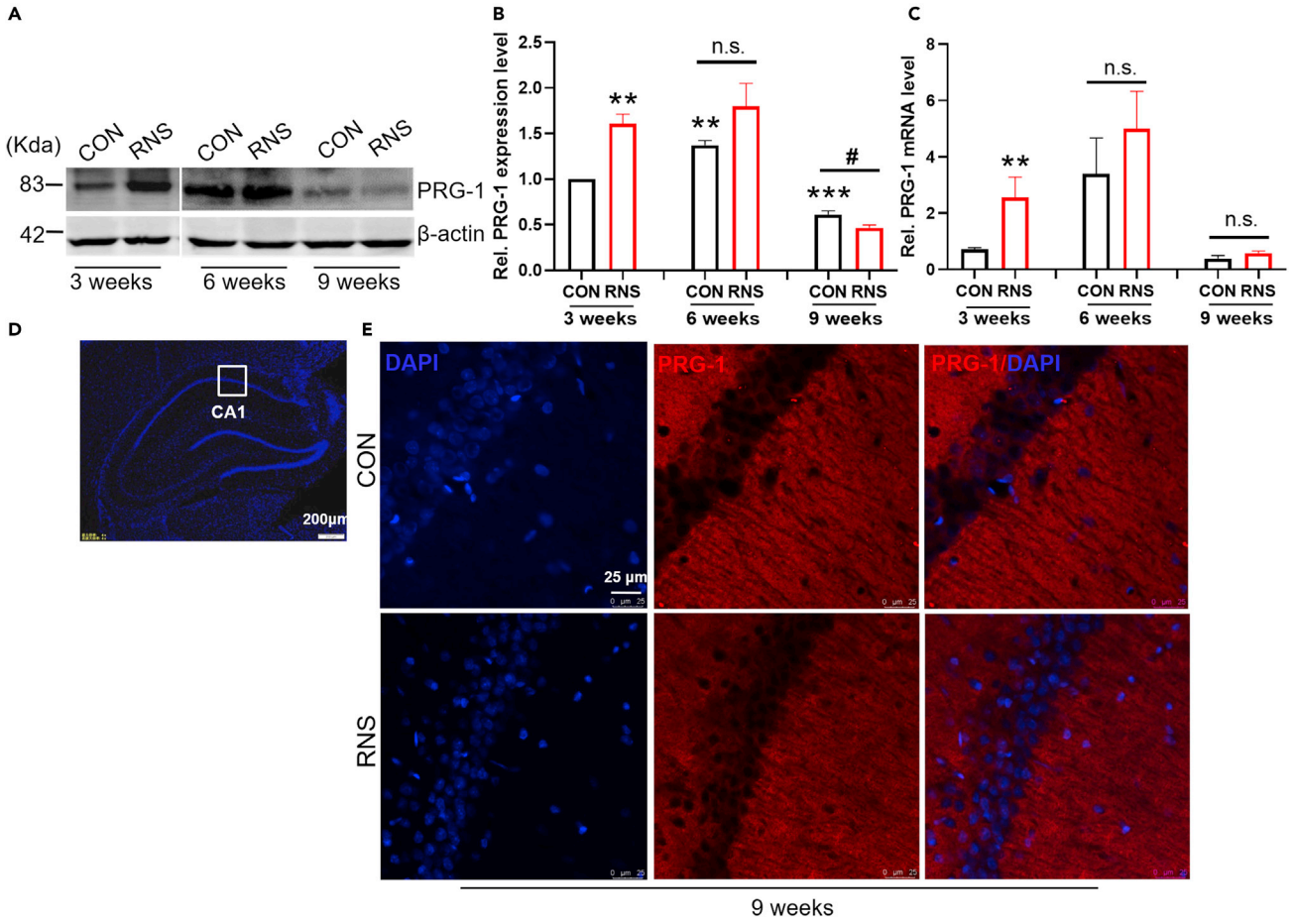

Figure 2. Hippocampal PRG-1 is involved in RNS-induced pain and behavioral impairments

(A and B) (A) Representative immunoblot and (B) quantitative analysis of gray values (normalized to CON group of 3 weeks) revealed that the expression levels of PRG-1 were increased at 3 weeks of age while decreased at 9 weeks in hippocampus of RNS rats compared with age-matched CON group (n = 6, **p < 0.01, ***p < 0.001 versus CON group of 3 weeks, one-sample t test; n.s. p > 0.05, #p < 0.05 versus age-matched CON group, two-tailed unpaired student t-test).

(C) Quantitative analysis of qRT-PCR showed that PRG-1 mRNA levels were increased at 3 weeks but not 6 or 9 weeks in the hippocampus of RNS rats. β-actin was included as a control (n = 6, n.s. p > 0.05, **p < 0.01 versus the corresponding CON group, two-tailed unpaired student t-test).

(D) DAPI overview of hippocampal section showing area of CA1 (highlighted by white square).

(E) Images of PRG-1 (red) and DAPI (blue) in the hippocampus from RNS and CON rats by immunofluorescence at 9 weeks (scale bar = 25 μm).

Data are expressed as mean ± SEM; RNS, repetitive noxious stimuli.

hippocampal PRG-1 expression was strongly increased at week 3, but decreased at 9 weeks of age in the RNS group (Figures 2A and 2B), indicating hippocampal PRG-1 may be involved in RNS-induced pain, learning, and memory impairment in childhood and adult, but has different mechanisms. Therefore, we focused at weeks 3 and 9 in our subsequent molecular studies.

In addition to protein content with Western blot, we measured PRG-1 mRNA in isolated hippocampus by qRT-PCR. Quantitative analysis showed that the PRG-1 mRNA was significantly increased in the hippocampus of RNS rats at 3 weeks but not at 6 or 9 weeks compared to the CON group at same timepoints (Figure 2C), suggesting that PRG-1 expression was specifically increased by transcription step in RNS rats. Furthermore, confocal microscopy indicated that subcellular PRG-1 is mainly expressed in the dendritic fields of the CA1, and further confirmed PRG-1 expression is low by adulthood in RNS rats at week 9 (Figures 2D and 2E). These data further suggested that PRG-1 could play different roles in childhood/juveniles, when synapses are still forming and maturing, and adults, when synaptic development is complete, in RNS-induced pain, learning, and memory impairment.

Decreased dendritic spine density in the hippocampus following neonatal RNS

Since it has been established that PRG-1 has a critical role in synaptic plasticity (Liu et al., 2016), we investigated the impact of neonatal RNS on hippocampal neuronal activity and dendritic spine density. Nissl staining was performed in the rats to examine nissl bodies and neuron damage in the hippocampus. We found that the hippocampus in CON group showed abundant nissl bodies in the cytoplasm and normal nucleoli in CA1 and DG regions. However, the hippocampus of RNS rats showed loss of nissl bodies and nucleoli at 3 weeks and 9 weeks, indicating damage of neuron (Figures 3A–3C).

We also compared spine densities of CON and RNS groups on week 3 and week 9 *in vivo* by Golgi-Cox staining to determine whether spine plasticity was associated with neonatal RNS treatment. The RNS rat group showed a significant decrease in spine density of 20%–30% in hippocampal CA1 (CA1 sr, CA1 so) and DG regions (moDG) (Figures 3D–3I) at 3 and 9 weeks, suggestion an important role of PRG-1 in RNS-induced pain, learning, and memory impairment via spine density regulation.

PRG-1 overexpression alleviated allodynia, learning, and memory impairment caused by neonatal RNS

Virus vectors LV-Plppr4 (to cause PRG-1 overexpression) or LV-Plppr4-RNAi (to silence PRG-1) were injected bilaterally into the hippocampus on week 3 (Figure 4A) to address the role of hippocampal PRG-1 in mediating changes caused by neonatal RNS. PRG-1 overexpression alleviated RNS-induced pain, including thermal hyperalgesia and mechanical allodynia (Figures 4B and 4C), and mitigated the impaired learning and memory impairment behaviors, including shortened escape latency time and less escape path length to target in spatial acquisition trials and more time in the quadrant zone in probe trials compared with RNS rats, in the rats by week 9 (Figures 4D–4F), while PRG-1 silencing caused aggravated pain (Figures 4B and 4C), indicating the analgesic and anti-learning and memory impairment effect of PRG-1 overexpression.

PRG-1 interacts with NSF to mediate RNS-induced pain

To uncover the mechanistic role of PRG-1 in modulating RNS-induced allodynia, we used a yeast two-hybrid system (Y2H) with PRG-1 C terminal domain (PRG-1 CD) as bait to identify putative interactors and the most promising candidate protein identified was NSF, which was found 18 times among the 40 prey sequences isolated. We confirmed a direct molecular interaction between PRG-1 and NSF using co-immunoprecipitation (CoIP) in adult rat hippocampus (Figure 5A). Interestingly, PRG-1/NSF interaction was inhibited in RNS rats compared with CON (Figure 5B), implying interaction of PRG-1 with NSF is involved in RNS-induced pain.

PRG-1/NSF interaction requires a.a. 346 located in the PRG-1 C-terminal domain

It was reported that a PRG-1 mutation in mice (R346T, which corresponds with R345T in human) leads to loss of PRG-1 function and is related to epileptic seizures (Vogt et al., 2016). To test whether this site serves as a critical residue for the putative interaction with NSF, HEK293 cells expressing wild-type PRG-1 or PRG-1-R346T were established. CoIP assays showed NSF can be co-immunoprecipitated with WT PRG-1 but not the PRG-1-R346T mutant (Figure 5C), implying that the R346 site is critical for PRG-1/NSF interaction.

ATP affects PRG-1/NSF interaction

ATP exerts multiple effects on synaptic plasticity and neuroglia interactions, as well as in mood disorders (Ma et al., 2018). To determine whether ATP is involved in the molecular interaction of PRG-1 with NSF, we applied ATP (100 μM, sigma) or a non-hydrolyzable ATP analog (ATPγS, 100 μM, sigma) to HEK293 cells expressing wild-type PRG-1 for 2 h (Figure 5D) and collected lysates for CoIP. We confirmed that ATP is involved in the interaction between PRG-1 and NSF because ATPγS enhanced this interaction while ATP decreased it (Figure 5D).

PRG-1/NSF interaction relieves allodynia, learning and memory impairment induced by neonatal RNS

Given that ATP decreases, while ATPγS enhances the PRG-1/NSF interaction, we next examined the physiological role of PRG-1 in mediating RNS-induced pain by administering multiple hippocampal microinjections of ATPγS (P60-62, 100 μM per day), which serves as an activator of PRG-1/NSF signaling, in the CON and RNS rat groups at week 9 (Figure 6A). ATPγS treatment led to a significant increase in TWL and MWT

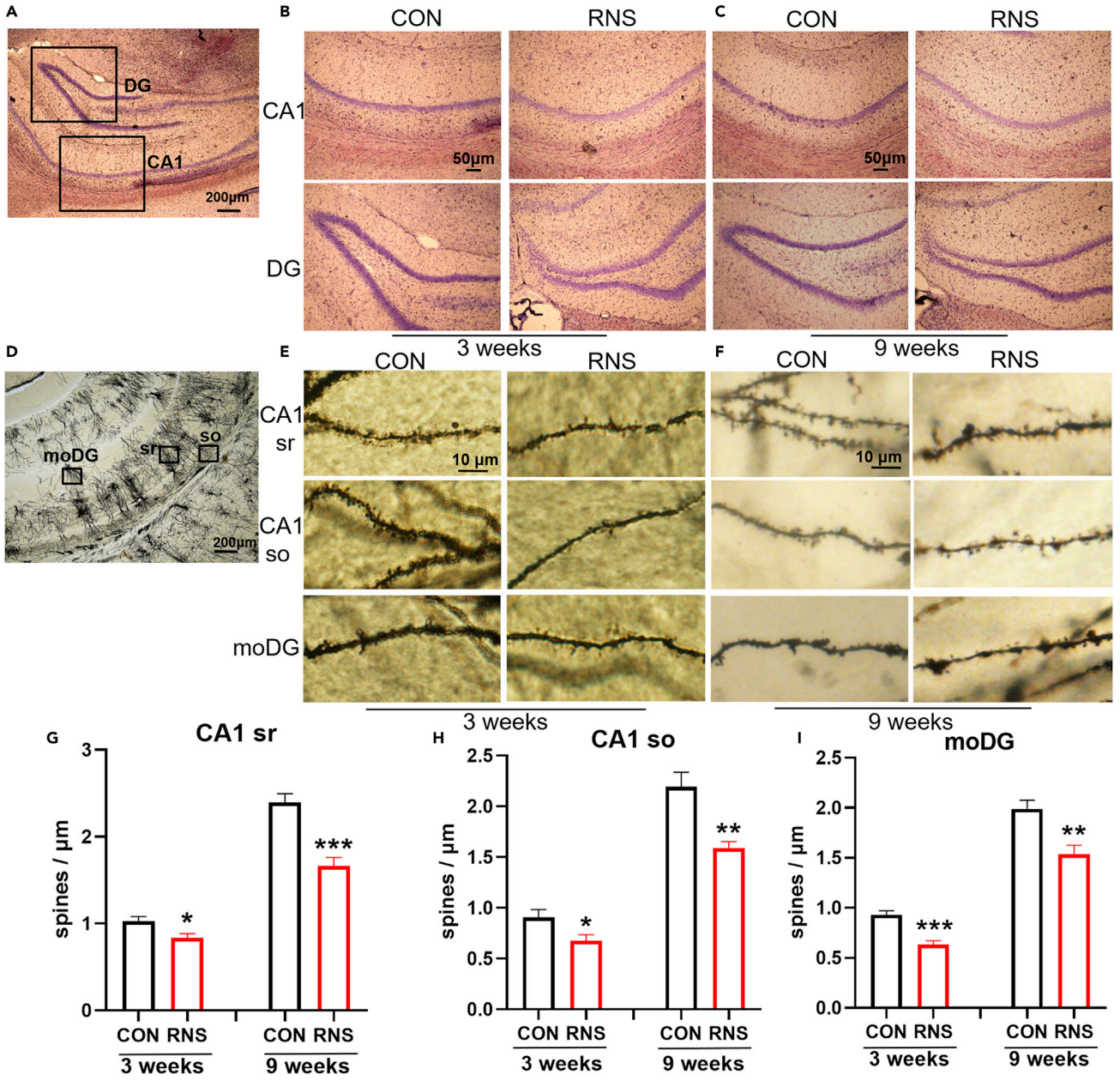

Figure 3. RNS rats display decreased spine density in the hippocampus

(A–C) (A) Nissl staining in whole hippocampus showing areas of CA1, DG zones. Nissl staining in CA1, DG regions of hippocampus at week 3 (B) and week 9 (C).

(D) Hippocampus showing areas of spine assessment (highlighted by black squares): stratum radiatum (sr, apical dendrites) and stratum oriens (so, basal dendrites) of the CA1 region, and the molecular layer of dentate gyri (moDG).

(E–I) (E and F) Golgi-Cox staining and (G-I) quantitative analysis showed that the spine density was decreased in the hippocampus of RNS rats. G, n = 11 CON and 8 RNS at 3 weeks, 12 CON and 11 RNS at 9 weeks; H, n = 12 CON and 9 RNS at 3 weeks, 12 CON and 9 RNS at 9 weeks; I, n = 12 CON and 10 RNS at 3 weeks, 12 CON and 8 RNS at 9 weeks; n represents analyzed dendritic segments; two-tailed unpaired student t test, *$p < 0.05$, **$p < 0.01$, ***$p < 0.001$ compared to the CON group at the same time point.

Data are expressed as mean ± SEM; RNS, repetitive noxious stimuli.

with cumulative effects in the RNS group (Figures 6B and 6C). ATPγS treatment also rescued learning and memory impairment by shortened escape latency time and less escape path length to target in spatial acquisition trials and more time in the quadrant zone in probe trials (Figures 6D–6F). Conversely, administration of ATP (P60-62, 100 μM per day), which should inhibit PRG-1/NSF signaling based on our cell

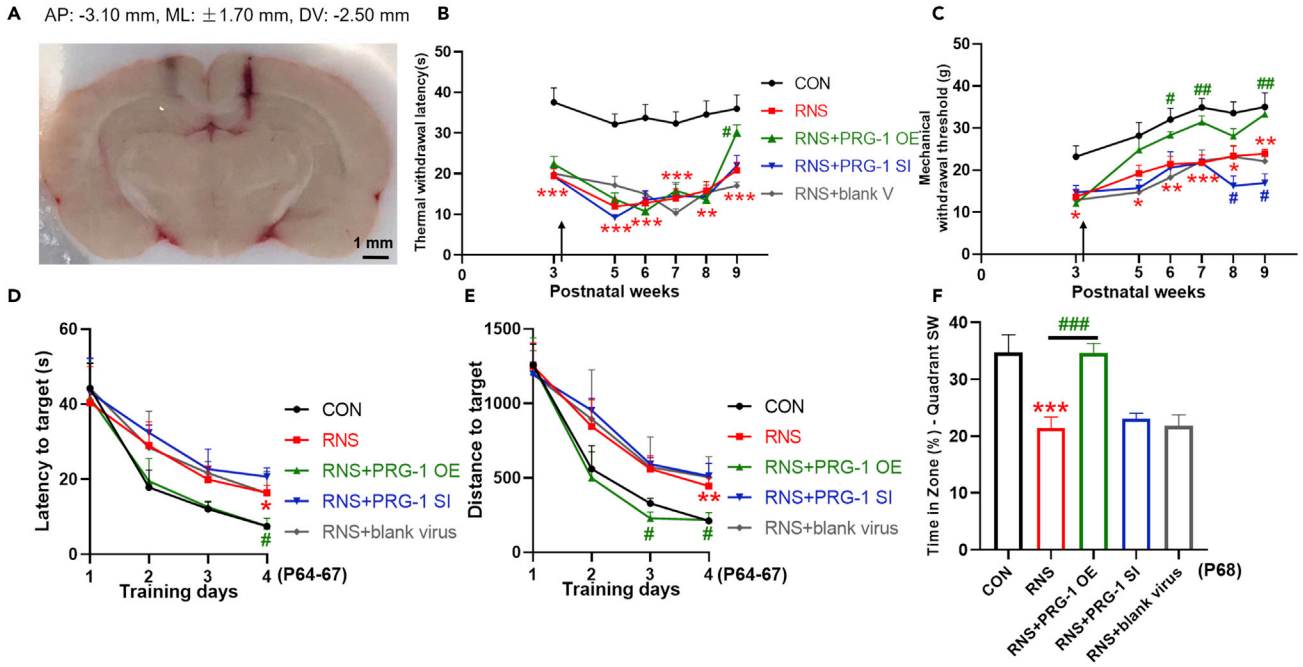

Figure 4. PRG-1 overexpression alleviated pain, learning, and memory impairments in RNS rats

(A) Schematic diagram of hippocampal microinjection in the rat models at week 3.

(B) Early hippocampus injection of virus vector LV-Plppr4 (PRG-1 OE) alleviated RNS-induced TWL decrease (n = 6; repeated measures two-way ANOVA with Tukey's post-hoc multiple comparisons test, *: vs CON group at the same time point; #: versus RNS group at the same time point); arrow indicates virus vector injection.

(C) Hippocampus injection of virus vector LV-Plppr4 (PRG-1 OE) alleviated RNS-induced MWT decrease while LV-Plppr4-RNAi (PRG-1 SI) lead to intensified pain (n = 6; repeated measures two-way ANOVA with Tukey's post-hoc multiple comparisons test, *: vs CON group at the same time point; #: vs RNS group at the same time point; arrow indicates virus vector injection).

(D-F) PRG-1 OE reversed the spatial learning and memory impairments in RNS rats by 9 weeks, such as shortened escape latency time to target (D), less escape path length to target (E) in spatial acquisition trials, and more time in the quadrant zone in probe trials (F) compared with RNS group (n = 6; D–E, repeated measures two-way ANOVA with Tukey's post-hoc multiple comparisons test; F, one-way ANOVA with Bonferroni post hoc; *: vs CON group at the same time point; #: vs RNS group at the same time point).

Data are presented as mean ± SEM with *p < 0.05, **p < 0.01, ***p < 0.001; RNS, repetitive noxious stimuli; TWL, thermal withdrawal latency; MWT, mechanical withdrawal threshold; OE, overexpression; SI, silencing.

studies, did not affect pain or learning and memory behaviors. These data suggested that PRG-1/NSF interaction relieves RNS-induced allodynia, learning, and memory impairment.

PRG-1/NSF relieves RNS-induced allodynia by reversing synaptic depression in the hippocampus

Next, we compared the effect of our PRG-1/NSF modulators on spine densities at week 9 *in vivo* by Golgi-Cox staining to determine whether PRG-1/NSF interaction is involved in regulating this process. Hippocampal microinjection of ATPγS or PRG-1 overexpression caused an increase in spine density compared with vehicle in hippocampus CA1 (sr and so) and moDG regions of the RNS rat group (Figures 7A–7D), further supporting the specific role of PRG-1 in spine density induced by RNS. These findings indicated that PRG-1/NSF may play analgesic and anti-memory impairment role by rescuing synaptic depression in the hippocampus of RNS rats.

PRG-1/NSF relieves RNS-induced pain in rats via glutamate secretion

After determining that hippocampal PRG-1/NSF is involved in mediating the RNS-induced impairments, we next determined the downstream neurotransmitter pathways involved. Glutamate is a major excitatory neurotransmitter of the central nervous system, and numerous studies have demonstrated the potential roles of the glutamatergic system in pain, learning, and memory disorders (Wang et al., 2015). Enzyme-linked immunosorbent assay (ELISA) analysis showed that secreted glutamate levels were increased in hippocampus of RNS rats at week 9 compared with age-matched CON group (Figure 8A). Furthermore, ATPγS

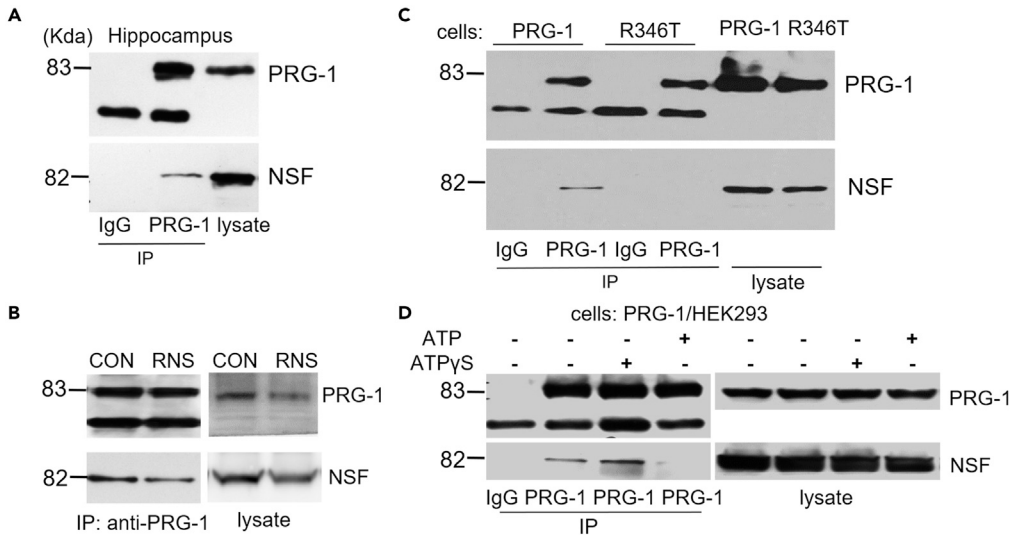

Figure 5. PRG-1 interacts with NSF

(A) CoIP using a PRG-1-specific antibody detected PRG-1/NSF interaction in the hippocampus.

(B) PRG-1/NSF interaction was inhibited in RNS rats compared with CON rats.

(C) CoIP using a PRG-1 antibody shows PRG-1 and NSF association in/HEK293 cells transfected with wild-type PRG-1, and that PRG-1-R346T mutation lost this interaction.

(D) Interaction between PRG-1 and NSF is enhanced by ATPγS (100 μM, 2 h) while decreased by ATP (100 μM, 2 h).

RNS, repetitive noxious stimuli; NSF, N-Ethylmaleimide sensitive fusion protein.

treatment or PRG-1 overexpression attenuated this increase in glutamate secretion (Figure 8B), suggesting that PRG-1/NSF relieves RNS-induced pain and impairments in rats via decreased glutamate release.

PRG-1/NSF relieves RNS-induced pain in rats via GluR2 signaling

To determine the effect of ATPγS treatment or PRG-1 overexpression on hippocampal expression of PRG-1, Western blot analysis was used which confirmed that PRG-1 protein levels were decreased in RNS rats compared with CON rats at week 9. Levels of PRG-1 in the RNS rats were restored to CON levels by PRG-1 overexpression but not ATPγS treatment (Figures 8C and 8D). To further examine the role of glutamatergic signaling in the RNS-induced impairments, we examined expression of AMPARs in the rats. AMPARs play a predominant role in excitatory synaptic transmission and plasticity. GluR2 is a key determinant of the biophysical properties of AMPARs among the four poreforming AMPAR subunits (GluR1–GluR4) (Greger et al., 2003).

Immunoblot analysis showed that GluR2 was decreased in the hippocampus of RNS rats compared with age-matched CON rats (Figures 8C and 8E), indicating changes in the composition of AMPAR subunits and the switch from GluR2-containing AMPARs to GluR2-lacking AMPARs at synapses. In line with PRG-1, GluR2 was also increased in the hippocampus of RNS rats following PRG-1 overexpression. However, GluR2 was increased by ATPγS comparing RNS rats. These data suggested that PRG-1/NSF relieves RNS-induced pain, learning, and memory impairments via decreased glutamate release and AMPAR GluR2 trafficking deficiency.

DISCUSSION

Analgesia management in neonates is challenging and often incorrect or over-looked completely. This can unfortunately have detrimental consequences since the infant stage is a critical period for CNS maturation and development of learning and memory. Clinical studies have shown that untreated pain in the NICU may developmentally impact the nervous system to cause adverse effects in short- and long-term brain development (Gaspardo et al., 2018; McPherson and Grunau, 2014; Mooney-Leber and Brummelte, 2017). These effects manifest as altered pain sensitivity and dysfunctional cognitive, emotional, and psychosocial sequelae later in life (Maxwell et al., 2019; Nuseir et al., 2021; Walker, 2019; Xia et al., 2020). Studies consistently show that appropriate stimulation in neonatal stage (e.g., breastfeeding, skin-to-skin care) can

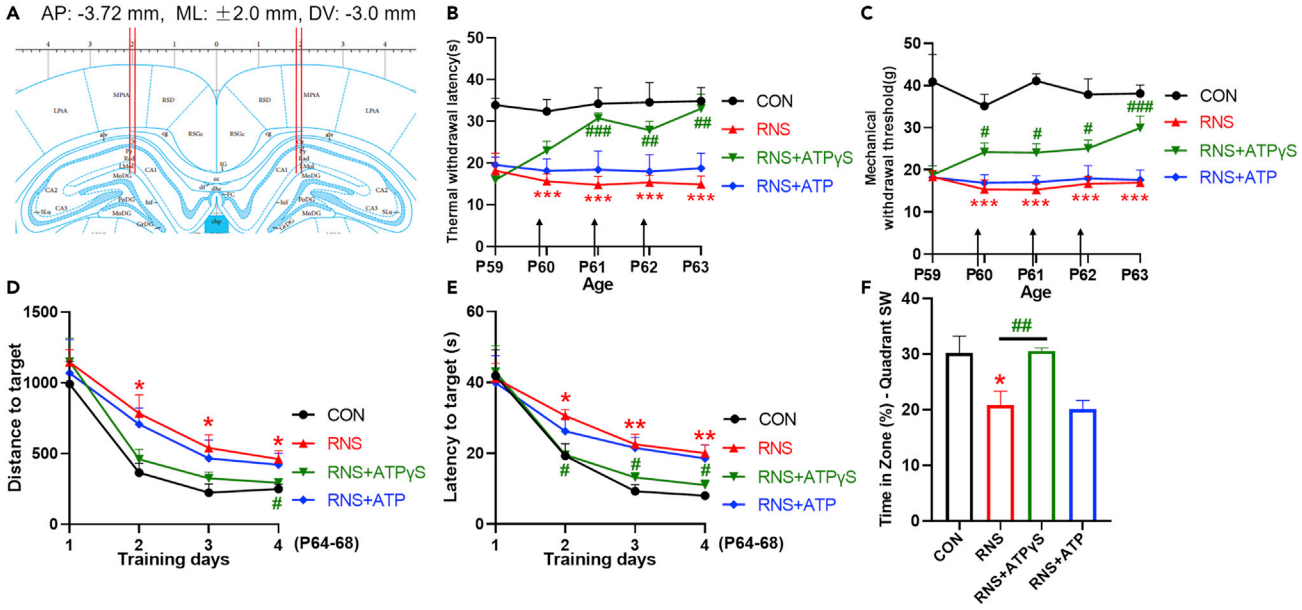

Figure 6. PRG-1/NSF interaction relieves allodynia, learning, and memory impairments in RNS rats

(A) Schematic diagram of hippocampal microinjection of adult rats (x = ±2.0 mm, y = −3.72 mm, and z = −3.0 mm).

(B) Chronic ATPγS (100 μM per day, P60-62) administration in adult rats (at 9 weeks) attenuated RNS-induced TWL impairments on P61-63 (n = 6; repeated measures two-way ANOVA with Tukey's post-hoc multiple comparisons test; *: vs CON group at the same time point; #: vs RNS group at the same time point; arrows indicate pharmacological treatment).

(C) Multiple ATPγS (100 μM per day, P60-62) administration attenuated RNS-induced MWT impairments on P60-63. (n = 6; repeated measures two-way ANOVA with Tukey's post-hoc multiple comparisons test; *: vs CON group at the same time point; #: vs RNS group at the same time point; arrows indicate pharmacological treatment).

(D–F) ATPγS reversed the spatial learning and memory impairments induced by RNS, and showed shortened escape latency time to target (D), less escape path length to target (E) in spatial acquisition trials, and more time in the quadrant zone in probe trials (F) compared with RNS group (n = 6; D-E, repeated measures two-way ANOVA with Tukey's post-hoc multiple comparisons test; F, one-way ANOVA with Bonferroni post hoc; *: vs CON group at the same time point; #: vs RNS group at the same time point).

Data are presented as mean ± SEM with *p < 0.05, **p < 0.01, ***p < 0.001; RNS, repetitive noxious stimuli; TWL, thermal withdrawal latency; MWT, mechanical withdrawal threshold.

increase hippocampal synapse density and promote healthy neurodevelopment, while excessively strong and long-term adverse stimuli during this stage (e.g., painful experiences, anesthetics exposure, and maternal separation) are associated with retarded brain responses. These suggest that early experiences may shape the somatosensory scaffolding responsible for directing perceptual, cognitive, and social development for later life (Chen et al., 2018; Maitre et al., 2017; Yu et al., 2018). Thus, clinical management of neonatal pain needs to take into consideration not only the modulation of acute behavioral and physiological responses but also the potential long-term effects of pain and injury (Walker, 2019). However, little is known regarding the mechanisms underlying the relationship between early pain experience on learning and memory formation later in life. To address these unknown questions, we established a neonatal RNS rat model to evaluate the impact of neonatal pain manipulation on later-life in the life cycle.

To date, studies on PRGs family have mainly focused on neuropsychiatric diseases and nerve injuries such as epilepsy (Ni et al., 2009; Trimbuch et al., 2009; Vogt et al., 2017), schizophrenia (Thalman et al., 2018; Vogt et al., 2016), memory disorders (Liu et al., 2016), nerve trauma (Hashimoto et al., 2013; Peeva et al., 2006), and sensory discrimination deficit (Cheng et al., 2016; Unichenko et al., 2016). We recently delineated a new physiological role for PRG-1 in chronic pain where we found that hippocampal PRG-1 relieves pain and depressive-like behaviors caused by bone cancer pain via $P2X_7R$/PRG-1/PP2A pathway regulation of dendritic spine density in a cell-autonomous fashion (Liu et al., 2021a). We also found that hippocampal PRG-1 expression was upregulated as a compensatory protective effect in response to the bone cancer-induced pain (Liu et al., 2021a).

In the present study, hippocampal PRG-1 was strongly increased at week 3 in rats after neonatal RNS but decreased by week 9. Neonatal RNS induced long-term pain hypersensitivity, loss of dendritic spines

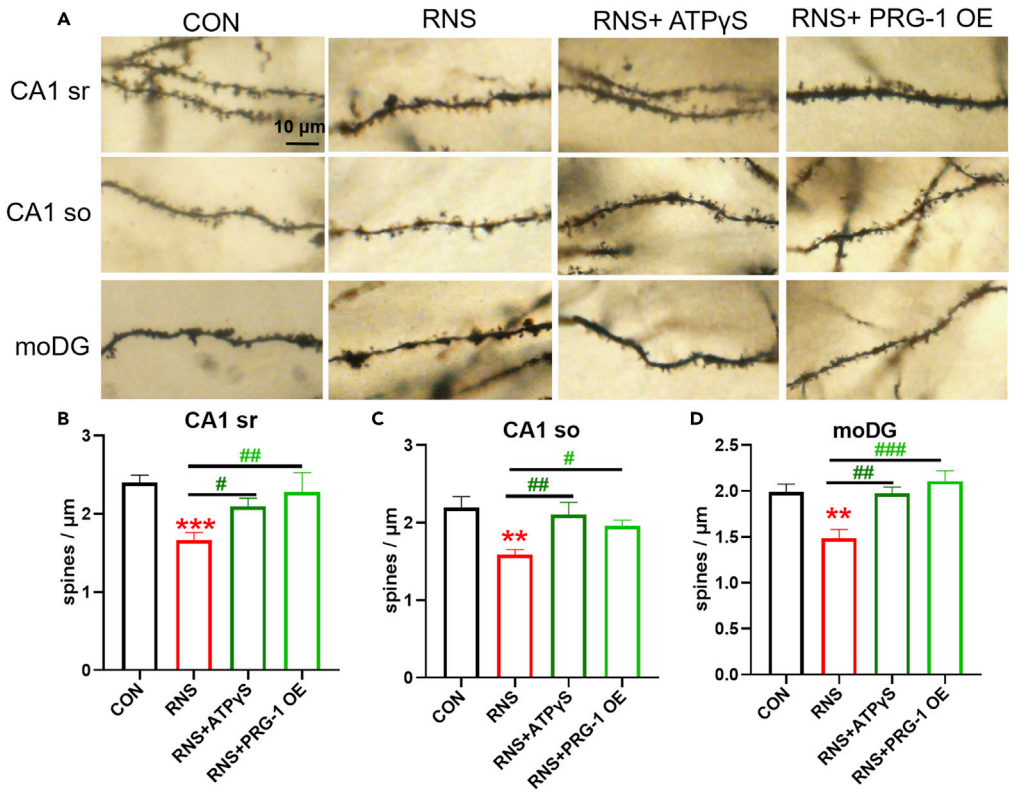

Figure 7. PRG-1/NSF relieves RNS-induced allodynia by reversing synaptic depression in the hippocampus

(A–D) (A) Images of Golgi-Cox staining and (B–D) quantitative analysis showing that the spine density depression induced by RNS was reversed by ATPγS and PRG-1 overexpression (B, n = 12 CON, 11 RNS, 11 RNS + ATPγS and 13 RNS + PRG-1 OE; C, n = 12 CON, 9 RNS, 14 RNS+ ATPγS and 10 RNS + PRG-1 OE; D, n = 12 CON, 8 RNS, 12 RNS+ ATPγS and 15 RNS + PRG-1 OE; B–D, one-way ANOVA with Bonferroni post hoc; n represents analyzed dendritic segments; *: vs CON group; #: vs RNS group). stratum radiatum (sr, apical dendrites) and stratum oriens (so, basal dendrites) of the CA1 region, and the molecular layer of dentate gyri (moDG).

Data are presented as mean ± SEM with *p < 0.05, **p < 0.01, ***p < 0.001; RNS, repetitive noxious stimuli.

density, learning, and memory deficiency in rats which persisted to adulthood in our experiment. These findings are similar to those of our previous findings (Liu et al., 2016), who observed dendritic spine damage and spatial memory dysfunction in PRG-1 knockout mice. These results indicate that neonatal RNS leads to decreased expression or hypofunction of PRG-1 in rats.

PRG-1 overexpression or PRG-1/NSF interaction enhanced by ATPγS enabled recovery of dendritic spine density in the hippocampal CA1 and DG regions following neonatal RNS, thereby alleviating the behavioral impairments, while PRG-1 silencing led to an intensified mechanical allodynia. Taken together, these reciprocal findings strongly suggest a role for hippocampal PRG-1 in the analgesic effects and relieving learning and memory impairments in rats after neonatal RNS.

However, one could argue that if PRG-1 does indeed play a protective role in neurodevelopment, it is unexpected that PRG-1 was strongly increased at week 3 following neonatal RNS. Such a response is not without precedent and indeed, compensatory adaptations can be found in all biological systems and is likely to be involved here, to some extent. Brauer et al. reported that after entorhinal cortex lesion, PRG-1 is significantly upregulated in all areas of the ipsilateral hippocampus one day after lesion (d.a.l) and peaks at 5 d.a.l, then is downregulated to control levels in 10–28 d.a.l (Brauer et al., 2003). A similar expression pattern was also seen in the contralateral hippocampus (1 d.a.l) and in the ipsilateral cortex (1–5 d.a.l) (Brauer et al., 2003). Similarly, PRG-1 also plays a compensatory protective role in brain injury caused by flurothyl-induced recurrent neonatal seizures (Ni et al., 2010). These findings suggest that PRG-1 expression following neonatal RNS in rats may be affected by a biphasic response to neonatal

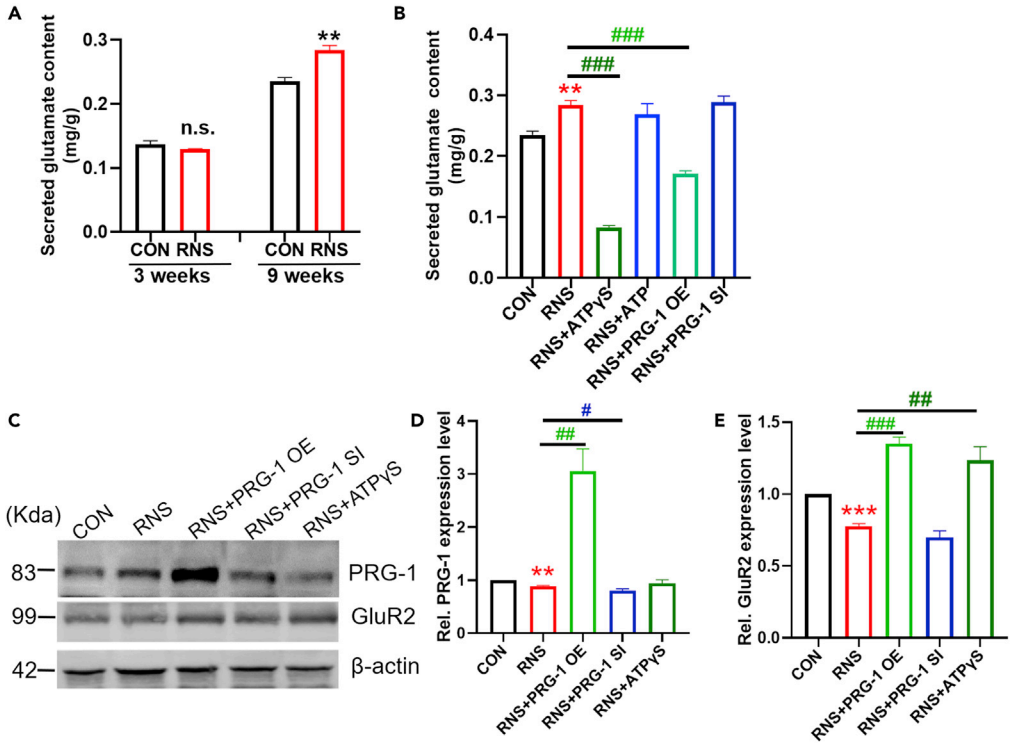

Figure 8. PRG-1/NSF relieves RNS-induced pain in rats via glutamine/GluR2 signaling

(A) Quantitative ELISA showing that secreted glutamate content was increased in hippocampus of RNS rats at 9 weeks compared with age-matched CON group (n = 6, two-tailed unpaired student t-test, *: vs CON group).

(B) Quantitative analysis showing that ATPγS or PRG-1 overexpression induced the secreted glutamate content decreased in hippocampus at 9 weeks in RNS rats (n = 6, one-way ANOVA with Bonferroni post hoc; *: vs CON group; #: vs RNS group).

(C–E) (C) Western blot and (D and E) quantitative analysis of gray values (normalized to CON values) showing PRG-1 and GluR2 expression in CON, RNS, RNS+ virus or drug group at 9 weeks (n = 6, *: vs CON group, D–E: one-sample t test. #: vs RNS group, D: one-way ANOVA with Bonferroni post hoc, E: Kruskal-Wallis test with a Dunn's multiple comparisons test). Data are presented as mean ± SEM with *p < 0.05, **p < 0.01, ***p < 0.001; RNS, repetitive noxious stimuli; OE, overexpression; SI, silencing.

RNS. Acutely, PRG-1 expression is downregulated by RNS in the neonatal period. PRG-1 expression is then temporarily upregulated following RNS due to compensatory protection in response to RNS-induced pain. The combination of these two factors leads to substantial up-regulation of PRG-1 expression in childhood (i.e., 3 weeks of age in rats). Over the subsequent few weeks, this self-protective effect weakens, leading to the decline of PRG-1 in the hippocampus by adulthood (i.e. 9 weeks of age).

Another interesting finding from the present study is that RNS rats at 3 weeks display higher PRG-1 expression while hippocampal spine densities and MWM performance are reduced. This may be partially due to the fact that spine densities and MWM performance are affected by a biphasic response to neonatal RNS. Initially, RNS-induced pain causes a sharp loss of hippocampal spine densities and a decline in MWM performance. In the second phase, higher PRG-1 concentrations caused by the compensatory response at 3 weeks are an attempt to mitigate the dendritic spine damage and relieve the pain and spatial memory dysfunction. In the absence of intervention, however, this second compensatory phase is weak under natural conditions. The combination of these two factors leads to reduced spine densities and MWM performance at 3 weeks. Interventions such as ectopic overexpression of PRG-1 or pharmacologic ATPγS administration to enhance PRG-1/NSF can normalize dendritic spine density and mitigate the pain and learning/memory deficiency induced by neonatal RNS.

This present study uncovered a previously unknown interaction of PRG-1 with NSF in hippocampus, and further dissected the role of PRG-1/NSF interaction in modulating RNS-induced impairments. NSF,

encoded by spontaneous recurrent epilepsy-related gene-1 (ERG1), is an ATPase known to play a key role in the release, docking, and fusion of synaptic vesicles, in addition to regulating the sorting, transport, and interaction of various neurotransmitter receptors on the postsynaptic membrane (Herold et al., 2018). ATP exerts multiple effects on synaptic plasticity and neuroglia interactions, as well as in mood disorders (Ma et al., 2018). Here, we confirmed the interaction between PRG-1 and NSF in ATP involved fashion, as the non-hydrolyzable analog of ATP, ATPγS enhanced PRG-1/NSF interaction while ATP blocked this interaction. Given that these reciprocal effects on PRG-1/NSF interaction also affect PRG-1 function, these findings suggest that PRG-1 may influence neuronal synaptic plasticity through interaction with NSF.

Glutamate is a major excitatory neurotransmitter of the central nervous system, and emerging studies have revealed previously unappreciated roles of the glutamatergic system in pain, learning, and memory disorders (Wang et al., 2015). One study showed that deletion of PRG-1 in mice caused increased LPA levels in the synaptic cleft and subsequent activation of LPA-2 receptors in presynaptic membrane, leading to a higher presynaptic glutamate release probability, hyperexcitability of cortical network and hippocampus, and ultimately epileptic seizures occurred (Trimbuch et al., 2009). To uncover the mechanisms by which PRG-1 modulates analgesia following neonatal RNS in rats, we examined the role of PRG-1/glutamate signaling in mediating RNS-induced impairments. We observed an increase in glutamate secretion in hippocampus of 9-week-old RNS rats compared with corresponding control group. Neonatal RNS-induced injury leads to inhibition of PRG-1 function, causing a higher presynaptic glutamate release. Furthermore, we also found that ATPγS treatment or PRG-1 overexpression in the hippocampus restored glutamate secretion in 9-week-old rats compared with RNS group, suggesting that PRG-1 prevents pain in RNS rats via diminished extracellular glutamate secretion.

AMPARs play a predominant role in excitatory synaptic transmission and plasticity. Among the four pore-forming AMPAR subunits (GluR1–GluR4), GluR2 is a key determinant of AMPARs biophysical properties (Greger et al., 2003). Most AMPARs in the adult brain consist of heteromeric GluR1/GluR2 subunits, which render AMPARs Ca^{2+} impermeable (CI-AMPARs) to maintain an appropriately low cytoplasmic Ca^{2+} level under physiological conditions (Li et al., 2021). Many neurological disorders show a switch from GluR2-containing CI-AMPARs to GluR2-lacking AMPARs at synapses, the latter being permeable to Ca^{2+} (CP-AMPARs) and dramatically altering synaptic function (Henley and Wilkinson, 2016). Our study found that on the one hand, neonatal RNS suppresses PRG-1 function and causes a higher extracellular presynaptic glutamate release. Simultaneously, neonatal RNS blocks PRG-1/NSF interaction and results in downregulated GluR2 expression in postsynaptic neuron, which could underlie a switch from GluR2-containing CI-AMPARs to GluR2-lacking CP-AMPARs in a cell-autonomous fashion, which may contribute to RNS-induced pain, learning, and memory impairment. In accordance with our findings, Chen et al. reported that the increased prevalence of postsynaptic GluR2-lacking CP-AMPARs, but not NMDARs, in the spinal dorsal horn contributes to the pathogenesis of streptozotocin-induced diabetic neuropathic pain (Chen et al., 2019). In addition, another report suggested that upregulation of GluR2-lacking CP-AMPARs could be a mechanism underlying synaptic plasticity dysfunction and cognitive deficits following neonatal sevoflurane exposure (Yu et al., 2018).

Neonatal maternal separation induced irritable bowel syndrome-like rats caused significantly enhanced expression of GluR2 but not GluR1, and facilitated LTP in the hippocampus, both of which contributed to visceral hypersensitvity in adulthood (Chen et al., 2017). Chronic melamine treatment impairs working memory and reduces prefrontal activity associated with inhibition of GluR2/3 subunit expression (Sun et al., 2021). Neonatal sevoflurane exposure in mice impaired learning and memory in adulthood, and reduced GluR1, 2, and 3 expressions in crude synaptosomal fractions from hippocampus (Liu et al., 2021c).

GluR1 CP-AMPARs are excluded basally from hippocampal CA1 synapses, while intracellular exposure to synaptotoxic β-amyloid (Aβ) (1–42) oligomers cause recruitment of CP-AMPARs to hippocampal CA1 synapses in Alzheimer disease (Whitcomb et al., 2015). The role of CP-AMPARs is plastic and strongly influenced by the inducing stimulus and by postnatal development (Purkey and Dell'Acqua, 2020). However, the roles of CP-AMPARs in controlling hippocampal plasticity remain controversial (Sanderson et al., 2021). Herein, neonatal RNS decreased GluR2 expression and changed hippocampal AMPAR composition to be GluR2-lacking, which may ultimately contribute to pain, learning, and memory impairments. GluR2 was increased by PRG-1 overexpression and ATPγS treatment in the hippocampus, reversing the change of AMPARs composition, suggesting the analgesic and anti-memory impairment effect of PRG-1 is mediated via Glu/GluR2 signaling.

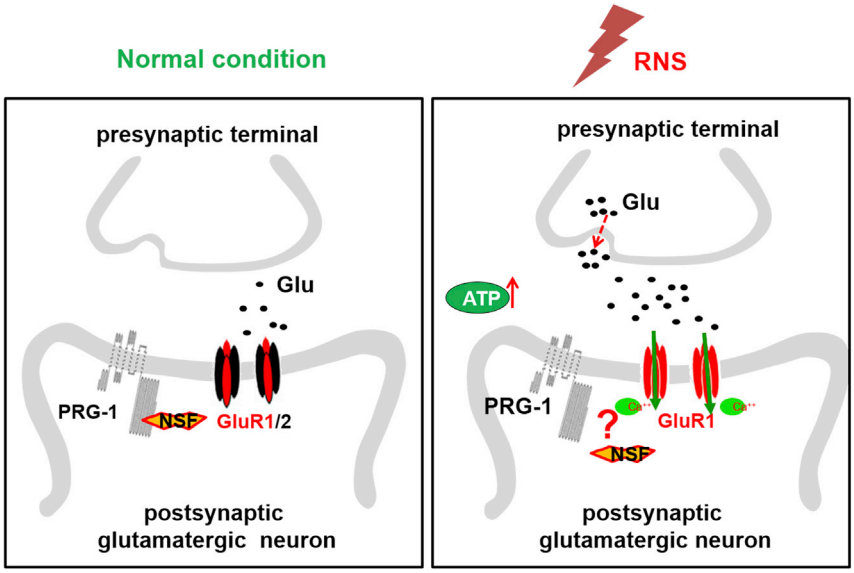

Figure 9. Schematic for the proposed mechanisms of PRG-1 modulating RNS-induced hyperalgesia, learning, and memory defects

Left: PRG-1/NSF interactions maintain PRG-1 function and neurotransmitter receptor stability under normal conditions. Right: Following neonatal RNS stress, the release of extracellular ATP is increased and further inhibits PRG-1 function and PRG-1/NSF interaction. Two pathways involving PRG-1 are initiated. On one pathway, inhibition of PRG-1 promotes the release of glutamate at the extracellular presynaptic membrane. Along the other pathway, PRG-1/NSF interaction interferes with the sorting, transport and interaction of neurotransmitter receptors, thus causing cell-autonomous AMPAR GluR2 trafficking deficiency, resulting in changes in synaptic activity, function, and structure. The two pathways modulate RNS-induced persistent hyperalgesia in a synergistic effect.

Calcium binding to calmodulin activates CaMKII, which leads to remodeling of the actin filament (F-actin) network in the spine (Wang et al., 2019). At low Ca^{2+} concentration, CaMKII binds to actin filaments and bundles them together, causing maturation and stabilization a rigid dendritic spine structure (Okamoto et al., 2007). At high Ca^{2+} concentration, Ca^{2+} binding to calmodulin triggers the dissociation of CaMKII from F-actin bundles (Wang et al., 2019). A small and short-term increase in glutamate or calcium allows dendritic spines to elongate, enlarge, and sprout new spines (Ucar et al., 2021). However, long periods and substantially increased glutamate or calcium concentration causes overactivation of PKC signaling, excitatory neural toxicity, and dendritic spines atrophy (Hains et al., 2009).

Collectively, our data suggest that neonatal RNS inhibits of PRG-1 function at postsynapses, causing glutamate release from presynaptic terminals, which then acts on glutamatergic receptors. At the same time, neonatal RNS blocks PRG-1/NSF interaction and causes GluR2 trafficking deficiency, which may switch GluR2-containing CI-AMPARs to GluR2-lacking CP-AMPARs on postsynapses of dendritic spine in hippocampal neurons. These simultaneous effects lead to postsynaptic Ca^{2+} influx, dendritic spine dysfunction, and ultimately contribute to pain, spatial learning, and memory deficits in adulthood (Figure 9). Additionally, temporary upregulation of PRG-1 provides a compensatory protective effect to mitigate RNS-induced pain.

Together with the functional and behavioral data, this study revealed that hippocampal PRG-1 signaling at postsynapses drives a synergistic effect of two different pathways in spine density regulation and subsequent RNS-induced pain, learning, and memory deficiency. These two pathways are comprised of presynaptic glutamate release and changes in postsynaptic neurons, as well as a cell-autonomous signaling pathway involving postsynaptic AMPARs regulation via PRG-1/NSF interaction. Furthermore, our studies identified a mechanism involving structural and functional synaptic changes in the hippocampus caused by defective GluR2 signaling which leads to behavioral impairments persisting until adulthood following neonatal RNS. We have also illustrated PRG-1 modulation as a drug target to mitigate RNS-induced impairments. In future, this may be important in preventing adverse effects of neonatal repetitive pain on brain development.

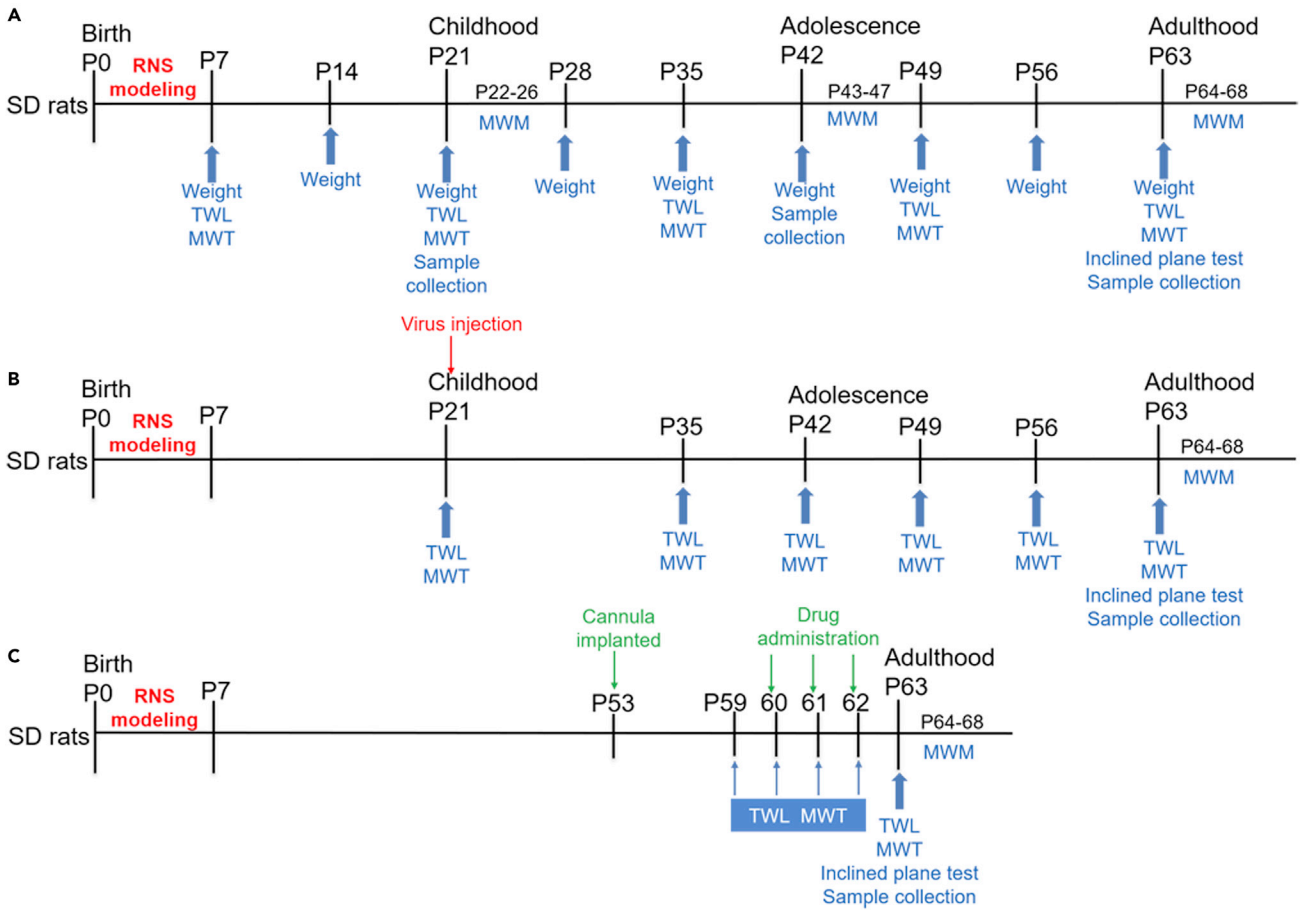

Figure 10. Schematic diagram of experimental design

(A) Blue arrows and words indicate the time of the behavior test and sample collection.

(B) Red arrow indicates the time of virus injection.

(C) Green arrows indicate the time of drug administration.

Limitations of the study

In the present study, only dendritic spine structure plasticity was analyzed in hippocampus, whereas electrophysiological characters of synaptic transmission, such as action potential rate, EPSC and LTP, were not been studied. Furthermore, differential roles of PRG-1 in RNS mediating hyperalgesia, learning, and memory dysfunction in different brain regions, such as PFC and ACC, need further investigation.

STAR★METHODS

Detailed methods are provided in the online version of this paper and include the following:

- KEY RESOURCES TABLE
- RESOURCE AVAILABILITY
  - Lead contact
  - Materials availability
  - Data and code availability
- EXPERIMENTAL MODEL AND SUBJECT DETAILS
  - Animals
  - Animal model of neonatal RNS
  - DNA constructs, cell culture, transfection, cell line establishment
- METHOD DETAILS
  - Implantation of hippocampal cannula and microinjection procedures

- Behavioral assessment
- Perfusion and immunofluorescence
- Co-immunoprecipitation (CoIP) and western blot (WB)
- Nissl staining
- Golgi-Cox staining and dendritic synapse quantification
- Enzyme-linked immunosorbent assay (ELISA) of glutamate
- RNA extraction and quantitative reverse transcription polymerase chain reaction (qRT-PCR)

- QUANTIFICATION AND STATISTICAL ANALYSIS

SUPPLEMENTAL INFORMATION

Supplemental information can be found online at https://doi.org/10.1016/j.isci.2022.104989.

ACKNOWLEDGMENTS

This work was supported by the National Natural Science Foundation of China (81960217, 81760214); Guizhou Provincial Science and Technology Planning Project (QianKeHe JiChu ZK[2021] 410); Major research project of innovation group in Education Department of Guizhou Province (QianJiaoHe KY[2017]043); the Doctoral Scientific Research Startup Fund Project of Zunyi Medical University (F-954).

AUTHOR CONTRIBUTIONS

Conceptualization, X.L., Z.X., and Y.T.; Methodology, X.L., S.L., W.Z., Z.X., J.H., and X.Z.; Investigation, X.L., S.L., Z.X., Y.T., S.Y., and S.C.; Writing – Original Draft, X.L. and S.L.; Writing – Review & Editing, Z.X., Y.T., S.Y., and S.C.; Funding Acquisition, X.L. and Z.X.; Resources, X.L. and Z.X.; Supervision, Z.X. and Y.T. All authors contributed to drafting or editing of parts of the manuscript and approved the final version of the manuscript.

DECLARATION OF INTERESTS

The authors declare no competing interests.

Received: May 6, 2022
Revised: July 2, 2022
Accepted: August 17, 2022
Published: September 16, 2022

REFERENCES

Anand, K.J., Coskun, V., Thrivikraman, K.V., Nemeroff, C.B., and Plotsky, P.M. (1999). Long-term behavioral effects of repetitive pain in neonatal rat pups. Physiol. Behav. *66*, 627–637. https://doi.org/10.1016/s0031-9384(98)00338-2.

Baxter, L., Moultrie, F., Fitzgibbon, S., Aspbury, M., Mansfield, R., Bastiani, M., Rogers, R., Jbabdi, S., Duff, E., and Slater, R. (2021). Functional and diffusion MRI reveal the neurophysiological basis of neonates' noxious-stimulus evoked brain activity. Nat. Commun. *12*, 2744. https://doi.org/10.1038/s41467-021-22960-0.

Bräuer, A.U., Savaskan, N.E., Kühn, H., Prehn, S., Ninnemann, O., and Nitsch, R. (2003). A new phospholipid phosphatase, PRG-1, is involved in axon growth and regenerative sprouting. Nat. Neurosci. *6*, 572–578. https://doi.org/10.1038/nn1052.

Cannavò, L., Perrone, S., Marseglia, L., Viola, V., Di Rosa, G., and Gitto, E. (2022). Potential benefits of melatonin to control pain in ventilated preterm newborns: an updated review. Pain Pract. *22*, 248–254. https://doi.org/10.1111/papr.13069.

Carbajal, R., Rousset, A., Danan, C., Coquery, S., Nolent, P., Ducrocq, S., Saizou, C., Lapillonne, A., Granier, M., Durand, P., et al. (2008). Epidemiology and treatment of painful procedures in neonates in intensive care units. JAMA *300*, 60–70. https://doi.org/10.1001/jama.300.1.60.

Chen, A., Chen, Y., Tang, Y., Bao, C., Cui, Z., Xiao, M., and Lin, C. (2017). Hippocampal AMPARs involve the central sensitization of rats with irritable bowel syndrome. Brain Behav. *7*, e00650. https://doi.org/10.1002/brb3.650.

Chen, S.R., Zhang, J., Chen, H., and Pan, H.L. (2019). Streptozotocin-induced diabetic neuropathic pain is associated with potentiated calcium-permeable AMPA receptor activity in the spinal cord. J. Pharmacol. Exp. Therapeut. *371*, 242–249. https://doi.org/10.1124/jpet.119.261339.

Chen, X., Zhou, X., Yang, L., Miao, X., Lu, D.H., Yang, X.Y., Zhou, Z.B., Kang, W.B., Chen, K.Y., Zhou, L.H., and Feng, X. (2018). Neonatal exposure to low-dose (1.2%) sevoflurane increases rats' hippocampal neurogenesis and synaptic plasticity in later life. Neurotox. Res. *34*, 188–197. https://doi.org/10.1007/s12640-018-9877-3.

Cheng, J., Sahani, S., Hausrat, T.J., Yang, J.W., Ji, H., Schmarowski, N., Endle, H., Liu, X., Li, Y., Böttche, R., et al. (2016). Precise somatotopic thalamocortical axon guidance depends on LPA-mediated PRG-2/radixin signaling. Neuron *92*, 126–142. https://doi.org/10.1016/j.neuron.2016.08.035.

Gaspardo, C.M., Cassiano, R.G.M., Gracioli, S.M.A., Furini, G.C.B., and Linhares, M.B.M. (2018). Effects of neonatal pain and temperament on attention problems in toddlers born preterm. J. Pediatr. Psychol. *43*, 342–351. https://doi.org/10.1093/jpepsy/jsx140.

Greger, I.H., Khatri, L., Kong, X., and Ziff, E.B. (2003). AMPA receptor tetramerization is mediated by Q/R editing. Neuron *40*, 763–774. https://doi.org/10.1016/s0896-6273(03)00668-8.

Hains, A.B., Vu, M.A.T., Maciejewski, P.K., van Dyck, C.H., Gottron, M., and Arnsten, A.F.T. (2009). Inhibition of protein kinase C signaling protects prefrontal cortex dendritic spines and cognition from the effects of chronic stress. Proc.

Natl. Acad. Sci. USA *106*, 17957–17962. https://doi.org/10.1073/pnas.0908563106.

Hargreaves, K., Dubner, R., Brown, F., Flores, C., and Joris, J. (1988). A new and sensitive method for measuring thermal nociception in cutaneous hyperalgesia. Pain *32*, 77–88.

Hashimoto, T., Yamada, M., Iwai, T., Saitoh, A., Hashimoto, E., Ukai, W., Saito, T., and Yamada, M. (2013). Plasticity-related gene 1 is important for survival of neurons derived from rat neural stem cells. J. Neurosci. Res. *91*, 1402–1407. https://doi.org/10.1002/jnr.23269.

Henley, J.M., and Wilkinson, K.A. (2016). Synaptic AMPA receptor composition in development, plasticity and disease. Nat. Rev. Neurosci. *17*, 337–350. https://doi.org/10.1038/nrn.2016.37.

Herold, C., Bidmon, H.J., Pannek, H.W., Hans, V., Gorji, A., Speckmann, E.J., and Zilles, K. (2018). ATPase N-ethylmaleimide-sensitive fusion protein: a novel key player for causing spontaneous network excitation in human temporal lobe epilepsy. Neuroscience *371*, 371–383. https://doi.org/10.1016/j.neuroscience.2017.12.013.

Hohmeister, J., Kroll, A., Wollgarten-Hadamek, I., Zohsel, K., Demirakça, S., Flor, H., and Hermann, C. (2010). Cerebral processing of pain in school-aged children with neonatal nociceptive input: an exploratory fMRI study. Pain *150*, 257–267. https://doi.org/10.1016/j.pain.2010.04.004.

Hoogen, N.J., Patijn, J., Tibboel, D., and Joosten, E.A. (2020). Repetitive noxious stimuli during early development affect acute and long-term mechanical sensitivity in rats. Pediatr. Res. *87*, 26–31. https://doi.org/10.1038/s41390-019-0420-x.

Huang, L., Wan, Y., Dang, Z., Yang, P., Yang, Q., and Wu, S. (2020). Hypoxic preconditioning ameliorated neuronal injury after middle cerebral artery occlusion by promoting neurogenesis. Brain Behav. *10*, e01804. https://doi.org/10.1002/brb3.1804.

Jones, L., Fabrizi, L., Laudiano-Dray, M., Whitehead, K., Meek, J., Verriotis, M., and Fitzgerald, M. (2017). Nociceptive cortical activity is dissociated from nociceptive behavior in newborn human infants under stress. Curr. Biol. *27*, 3846–3851.e3. https://doi.org/10.1016/j.cub.2017.10.063.

Knaepen, L., Patijn, J., van Kleef, M., Mulder, M., Tibboel, D., and Joosten, E.A.J. (2013). Neonatal repetitive needle pricking: plasticity of the spinal nociceptive circuit and extended postoperative pain in later life. Dev. Neurobiol. *73*, 85–97. https://doi.org/10.1002/dneu.22047.

Li, L., Chen, S.R., Zhou, M.H., Wang, L., Li, D.P., Chen, H., Lee, G., Jayaraman, V., and Pan, H.L. (2021). Alpha 2 delta-1 switches the phenotype of synaptic AMPA receptors by physically disrupting heteromeric subunit assembly. Cell Rep. *36*, 109396. https://doi.org/10.1016/j.celrep.2021.109396.

Li, P., Zhang, Q., Xiao, Z., Yu, S., Yan, Y., and Qin, Y. (2018). Activation of the P2X7 receptor in midbrain periaqueductal gray participates in the analgesic effect of tramadol in bone cancer pain rats. Mol. Pain *14*. 1744806918803039–14. https://doi.org/10.1177/1744806918803039.

Liu, X., Huai, J., Endle, H., Schlüter, L., Fan, W., Li, Y., Richers, S., Yurugi, H., Rajalingam, K., Ji, H., et al. (2016). PRG-1 regulates synaptic plasticity via intracellular PP2A/beta1-Integrin signaling. Dev. Cell *38*, 275–290. https://doi.org/10.1016/j.devcel.2016.06.019.

Liu, X., Xie, Z., Li, S., He, J., Cao, S., and Xiao, Z. (2021a). PRG-1 relieves pain and depressive-like behaviors in rats of bone cancer pain by regulation of dendritic spine in hippocampus. Int. J. Biol. Sci. *17*, 4005–4020. https://doi.org/10.7150/ijbs.59032.

Liu, X., He, J., and Xiao, Z. (2021b). Neurotropin alleviates rat osteocarcinoma pain via P2X3 receptor activation in the midbrain periaqueductal gray. Iran. J. Basic Med. Sci. *24*, 1395–1403. https://doi.org/10.22038/ijbms.2021.57965.12904.

Liu, Y., Yang, H., Fu, Y., Pan, Z., Qiu, F., Xu, Y., Yang, X., Chen, Q., Ma, D., and Liu, Z. (2021c). TRPV1 antagonist prevents neonatal sevoflurane-induced synaptic abnormality and cognitive impairment in mice through regulating the src/cofilin signaling pathway. Front. Cell Dev. Biol. *9*, 684516. https://doi.org/10.3389/fcell.2021.684516.

Luo, T., Yu, S., Cai, S., Zhang, Y., Jiao, Y., Yu, T., and Yu, W. (2018). Parabrachial neurons promote behavior and electroencephalographic arousal from general anesthesia. Front. Mol. Neurosci. *11*, 420. https://doi.org/10.3389/fnmol.2018.00420.

Ma, J., Qi, X., Yang, C., Pan, R., Wang, S., Wu, J., Huang, L., Chen, H., Cheng, J., Wu, R., et al. (2018). Calhm2 governs astrocytic ATP releasing in the development of depression-like behaviors. Mol. Psychiatr. *23*, 883–891. https://doi.org/10.1038/mp.2017.229.

Maitre, N.L., Key, A.P., Chorna, O.D., Slaughter, J.C., Matusz, P.J., Wallace, M.T., and Murray, M.M. (2017). The dual nature of early-life experience on somatosensory processing in the human infant brain. Curr. Biol. *27*, 1048–1054. https://doi.org/10.1016/j.cub.2017.02.036.

Maxwell, L.G., Fraga, M.V., and Malavolta, C.P. (2019). Assessment of pain in the newborn: an update. Clin. Perinatol. *46*, 693–707. https://doi.org/10.1016/j.clp.2019.08.005.

McPherson, C., and Grunau, R.E. (2014). Neonatal pain control and neurologic effects of anesthetics and sedatives in preterm infants. Clin. Perinatol. *41*, 209–227. https://doi.org/10.1016/j.clp.2013.10.002.

Mogil, J.S. (2009). Animal models of pain: progress and challenges. Nat. Rev. Neurosci. *10*, 283–294. https://doi.org/10.1038/nrn2606.

Mooney-Leber, S.M., and Brummelte, S. (2017). Neonatal pain and reduced maternal care: early-life stressors interacting to impact brain and behavioral development. Neuroscience *342*, 21–36. https://doi.org/10.1016/j.neuroscience.2016.05.001.

Ni, H., Jiang, Y.W., Tao, L.Y., Jin, M.F., and Wu, X.R. (2009). ZnT-1, ZnT-3, CaMK II, PRG-1 expressions in hippocampus following neonatal seizure-induced cognitive deficit in rats. Toxicol. Lett. *184*, 145–150. https://doi.org/10.1016/j.toxlet.2008.11.003.

Ni, H., Jiang, Y.W., Xiao, Z.J., Tao, L.Y., Jin, M.F., and Wu, X.R. (2010). Dynamic pattern of gene expression of ZnT-1, ZnT-3 and PRG-1 in rat brain following flurothyl-induced recurrent neonatal seizures. Toxicol. Lett. *194*, 86–93. https://doi.org/10.1016/j.toxlet.2010.02.008.

Nuseir, K.Q., Alzoubi, K.H., Alhusban, A.Y., Alazzani, M., Bawaane, A., and Khabour, O.F. (2021). Saccharin and naltrexone prevent increased pain sensitivity and impaired long-term memory induced by repetitive neonatal noxious stimulation: role of BDNF and enkephalin. Naunyn-Schmiedebergs Arch. Pharmacol. *394*, 1641–1650. https://doi.org/10.1007/s00210-021-02086-2.

Okamoto, K.I., Narayanan, R., Lee, S.H., Murata, K., and Hayashi, Y. (2007). The role of CaMKII as an F-actin-bundling protein crucial for maintenance of dendritic spine structure. Proc. Natl. Acad. Sci. USA *104*, 6418–6423. https://doi.org/10.1073/pnas.0701656104.

Paxinos, G., and Watson, C. (2007). The Rat Brain in Stereotaxic Coordinates, Sixth Edition (Academic Press).

Peeva, G.P., Angelova, S.K., Guntinas-Lichius, O., Streppel, M., Irintchev, A., Schütz, U., Popratiloff, A., Savaskan, N.E., Bräuer, A.U., Alvanou, A., et al. (2006). Improved outcome of facial nerve repair in rats is associated with enhanced regenerative response of motoneurons and augmented neocortical plasticity. Eur. J. Neurosci. *24*, 2152–2162. https://doi.org/10.1111/j.1460-9568.2006.05091.x.

Peters, J.W.B., Schouw, R., Anand, K.J.S., van Dijk, M., Duivenvoorden, H.J., and Tibboel, D. (2005). Does neonatal surgery lead to increased pain sensitivity in later childhood? Pain *114*, 444–454. https://doi.org/10.1016/j.pain.2005.01.014.

Purkey, A.M., and Dell'Acqua, M.L. (2020). Phosphorylation-dependent regulation of Ca2+-permeable AMPA receptors during hippocampal synaptic plasticity. Front. Synaptic Neurosci. *12*, 8. https://doi.org/10.3389/fnsyn.2020.00008.

Ranger, M., and Grunau, R.E. (2014). Early repetitive pain in preterm infants in relation to the developing brain. Pain Manag. *4*, 57–67. https://doi.org/10.2217/pmt.13.61.

Rivlin, A.S., and Tator, C.H. (1977). Objective clinical assessment of motor function after experimental spinal cord injury in the rat. J. Neurosurg. *47*, 577–581.

Sanderson, J.L., Freund, R.K., Gorski, J.A., and Dell'Acqua, M.L. (2021). beta-Amyloid disruption of LTP/LTD balance is mediated by AKAP150-anchored PKA and Calcineurin regulation of Ca2+-permeable AMPA receptors. Cell Rep. *37*, 109786. https://doi.org/10.1016/j.celrep.2021.109786.

Schwaller, F., and Fitzgerald, M. (2014). The consequences of pain in early life: injury-induced plasticity in developing pain pathways. Eur. J. Neurosci. *39*, 344–352. https://doi.org/10.1111/ejn.12414.

Slater, R., Fabrizi, L., Worley, A., Meek, J., Boyd, S., and Fitzgerald, M. (2010). Premature infants display increased noxious-evoked neuronal

activity in the brain compared to healthy age-matched term-born infants. Neuroimage *52*, 583–589. https://doi.org/10.1016/j.neuroimage.2010.04.253.

Strauss, U., and Bräuer, A.U. (2013). Current views on regulation and function of plasticity-related genes (PRGs/LPPRs) in the brain. Biochim. Biophys. Acta *1831*, 133–138. https://doi.org/10.1016/j.bbalip.2012.08.010.

Sun, W., Tang, D., Yang, Y., Wu, Z., Li, X., and An, L. (2021). Melamine impairs working memory and reduces prefrontal activity associated with inhibition of AMPA receptor GluR2/3 subunit expression. Toxicol. Lett. *350*, 171–184. https://doi.org/10.1016/j.toxlet.2021.07.009.

Thalman, C., Horta, G., Qiao, L., Endle, H., Tegeder, I., Cheng, H., Laube, G., Sigurdsson, T., Hauser, M.J., Tenzer, S., et al. (2018). Synaptic phospholipids as a new target for cortical hyperexcitability and E/I balance in psychiatric disorders. Mol. Psychiatr. *23*, 1699–1710. https://doi.org/10.1038/s41380-018-0053-1.

Theer, P., Mongis, C., and Knop, M. (2014). PSFj: know your fluorescence microscope. Nat. Methods *11*, 981–982. https://doi.org/10.1038/nmeth.3102.

Tokumitsu, H., Hatano, N., Tsuchiya, M., Yurimoto, S., Fujimoto, T., Ohara, N., Kobayashi, R., and Sakagami, H. (2010). Identification and characterization of PRG-1 as a neuronal calmodulin-binding protein. Biochem. J. *431*, 81–91. https://doi.org/10.1042/BJ20100637.

Trimbuch, T., Beed, P., Vogt, J., Schuchmann, S., Maier, N., Kintscher, M., Breustedt, J., Schuelke, M., Streu, N., Kieselmann, O., et al. (2009). Synaptic PRG-1 modulates excitatory transmission via lipid phosphate-mediated signaling. Cell *138*, 1222–1235. https://doi.org/10.1016/j.cell.2009.06.050.

Ucar, H., Watanabe, S., Noguchi, J., Morimoto, Y., Iino, Y., Yagishita, S., Takahashi, N., and Kasai, H. (2021). Mechanical actions of dendritic-spine enlargement on presynaptic exocytosis. Nature *600*, 686–689. https://doi.org/10.1038/s41586-021-04125-7.

Unichenko, P., Kirischuk, S., Yang, J.W., Baumgart, J., Roskoden, T., Schneider, P., Sommer, A., Horta, G., Radyushkin, K., Nitsch, R., et al. (2016). Plasticity-related gene 1 affects mouse barrel cortex function via strengthening of glutamatergic thalamocortical transmission. Cerebr. Cortex *26*, 3260–3272. https://doi.org/10.1093/cercor/bhw066.

Verriotis, M., Chang, P., Fitzgerald, M., and Fabrizi, L. (2016). The development of the nociceptive brain. Neuroscience *338*, 207–219. https://doi.org/10.1016/j.neuroscience.2016.07.026.

Vivancos, G.G., Verri, W.A., Jr., Cunha, T.M., Schivo, I.R.S., Parada, C.A., Cunha, F.Q., and Ferreira, S.H. (2004). An electronic pressure-meter nociception paw test for rats. Braz. J. Med. Biol. Res. *37*, 391–399. https://doi.org/10.1590/s0100-879x2004000300017.

Vogt, J., Kirischuk, S., Unichenko, P., Schlüter, L., Pelosi, A., Endle, H., Yang, J.W., Schmarowski, N., Cheng, J., Thalman, C., et al. (2017). Synaptic phospholipid signaling modulates axon outgrowth via glutamate-dependent Ca2+-mediated molecular pathways. Cerebr. Cortex *27*, 131–145. https://doi.org/10.1093/cercor/bhw370.

Vogt, J., Yang, J.W., Mobascher, A., Cheng, J., Li, Y., Liu, X., Baumgart, J., Thalman, C., Kirischuk, S., Unichenko, P., et al. (2016). Molecular cause and functional impact of altered synaptic lipid signaling due to a prg-1 gene SNP. EMBO Mol. Med. *8*, 25–38. https://doi.org/10.15252/emmm.201505677.

Vorhees, C.V., and Williams, M.T. (2006). Morris water maze: procedures for assessing spatial and related forms of learning and memory. Nat. Protoc. *1*, 848–858. https://doi.org/10.1038/nprot.2006.116.

Walker, S.M. (2019). Long-term effects of neonatal pain. Semin. Fetal Neonatal Med. *24*, 101005. https://doi.org/10.1016/j.siny.2019.04.005.

Wan, J., Shen, C.M., Wang, Y., Wu, Q.Z., Wang, Y.L., Liu, Q., Sun, Y.M., Cao, J.P., and Wu, Y.Q. (2021). Repeated exposure to propofol in the neonatal period impairs hippocampal synaptic plasticity and the recognition function of rats in adulthood. Brain Res. Bull. *169*, 63–72. https://doi.org/10.1016/j.brainresbull.2021.01.007.

Wang, Q., Chen, M., Schafer, N.P., Bueno, C., Song, S.S., Hudmon, A., Wolynes, P.G., Waxham, M.N., and Cheung, M.S. (2019). Assemblies of calcium/calmodulin-dependent kinase II with actin and their dynamic regulation by calmodulin in dendritic spines. Proc. Natl. Acad. Sci. USA *116*, 18937–18942. https://doi.org/10.1073/pnas.1911452116.

Wang, X.Q., Zhong, X.L., Li, Z.B., Wang, H.T., Zhang, J., Li, F., Zhang, J.Y., Dai, R.P., Xin-Fu, Z., Li, C.Q., et al. (2015). Differential roles of hippocampal glutamatergic receptors in neuropathic anxiety-like behavior after partial sciatic nerve ligation in rats. BMC Neurosci. *16*, 14. https://doi.org/10.1186/s12868-015-0150-x.

Whitcomb, D.J., Hogg, E.L., Regan, P., Piers, T., Narayan, P., Whitehead, G., Winters, B.L., Kim, D.H., Kim, E., St George-Hyslop, P., et al. (2015). Intracellular oligomeric amyloid-beta rapidly regulates GluA1 subunit of AMPA receptor in the hippocampus. Sci. Rep. *5*, 10934. https://doi.org/10.1038/srep10934.

Xia, D., Min, C., Chen, Y., Ling, R., Chen, M., and Li, X. (2020). Repetitive pain in neonatal male rats impairs hippocampus-dependent fear memory later in life. Front. Neurosci. *14*, 722. https://doi.org/10.3389/fnins.2020.00722.

Yu, X., Zhang, F., and Shi, J. (2018). Neonatal exposure to sevoflurane caused cognitive deficits by dysregulating SK2 channels and GluA2-lacking AMPA receptors in juvenile rat hippocampus. Neuropharmacology *141*, 66–75. https://doi.org/10.1016/j.neuropharm.2018.08.014.

Zhao, M., Wang, W., Jiang, Z., Zhu, Z., Liu, D., Pan, F., and biology, d. (2020). Long-term effect of post-traumatic stress in adolescence on dendrite development and H3K9me2/BDNF expression in male rat Hippocampus and prefrontal cortex. Front. Cell Dev. Biol. *8*, 682. https://doi.org/10.3389/fcell.2020.00682.

Zimmermann, M. (1983). Ethical guidelines for investigations of experimental pain in conscious animals. Pain *16*, 109–110. https://doi.org/10.1016/0304-3959(83)90201-4.

STAR★METHODS

KEY RESOURCES TABLE

REAGENT or RESOURCE	SOURCE	IDENTIFIER
Antibodies		
PRG-1	synaptic system	Cat# 282002; RRID: AB_2620015
normal rabbit IgG	Millipore	Cat# 12-370; RRID: AB_145841
GluR2	Novus	Cat# ab206293; RRID: AB_2800401
NSF	Abcam	Cat# ab126202; RRID: AB_11128656
ß-actin	MP Biomedicals	Cat# 691001; RRID: AB_2335127
Bacterial and virus strains		
LV-Plppr4	Genechem	ID: LV-Plppr4(47472-1)
LV-Plppr4-RNAi	Genechem	ID: Plppr4-RNAi(85438-1)
Chemicals, peptides, and recombinant proteins		
ATPγS	Sigma	A1388-1MG
ATP	Sigma	20-306
Experimental models: Cell lines		
HEK293	SIBS Cellbank	GNHu43
Oligonucleotides		
Primers for PRG-1, ß-actin, see Table S2	This paper	N/A
Recombinant DNA		
pIRESneo3-PRG-1	This paper	N/A
pIRESneo3-PRG-1-R346T	This paper	N/A
Software and algorithms		
Smart 3.0 system	Panlab	https://www.harvardapparatus.com/smart-video-tracking-system.html
Image J 6.0 software	NIH	https://imagej.nih.gov/ij/
GraphPad Prism (version 8.0.2)	GraphPad Software, Inc.	https://www.graphpad.com/

RESOURCE AVAILABILITY

Lead contact

Further information and requests for resources and reagents should be directed to and will be fulfilled by the lead contact, Zhi Xiao (zhixiao@zmu.edu.cn).

Materials availability

Virus generated in this study have been deposited to Genechem, LV-Plppr4, ID: LV-Plppr4(47472-1); Plppr4-RNAi, ID: Plppr4-RNAi(85438-1).

This study did not generate new unique reagents.

Data and code availability

- The data reported in this paper will be shared by the lead contact upon request.
- This paper does not report original code.
- Any additional information required to reanalyze the data reported in this paper is available from the lead contact upon request.

EXPERIMENTAL MODEL AND SUBJECT DETAILS

Animals

Pathogen-free Sprague–Dawley (SD) rats weighing 250 ± 10 g were purchased from the Tianqin Biotechnology Co. Ltd. (license number: SCXK (xiang) 2019-0014; Changsha, China) and lines were maintained via normal breeding. A total of n = 270 rat pups (both male and female) were used for all experiments. Rats were housed in a temperature (23 ± 2°C) and humidity (55 ± 5%) -controlled environment, with a 12-h light/dark cycle (8:00 a.m.–8:00 p.m.) and *ad libitum* access to food and water. All experimental procedures were in accordance with the guidelines of the Ethical Committee of the International Association for the Study of Pain (IASP) (Zimmermann, 1983) and ethically approved by the Animal Care Ethics Committee of Zunyi Medical University (zunyilunshen [2020] 2–098). All viable efforts were made to minimize the use of animals and reduce their suffering from experimental procedures.

Overall experimental design is shown in the schematic diagram (Figure 10). The grouping and number of rats are shown in Table S1. A total of 120 rats were used in the first part of the experiment: control (CON) group (n = 60), RNS group (n = 60) for behavioral test, and 6 rats at 3 weeks (childhood), 6 rats at 6 weeks (adolescence) and 6 rats at 9 weeks (adulthood) in each group were used for CoIP, western blots and RT-PCR. Then, 6 rats at 3 weeks and 6 rats at 9 weeks in each group were used for Golgi staining, 6 rats at 3 weeks and 6 rats at 9 weeks in each group were used for ELISA. Finally, 6 rats at 3 weeks and 6 rats at 9 weeks were used for nissl staining and immunofluorescence (IF). There were 150 rats in the second part of the experiment: CON group (n = 24), RNS group (n = 24), RNS +ATPγS group (n = 24), RNS +ATP group (n = 24), RNS +PRG-1 overexpression (OE) group (n = 24), RNS +PRG-1 silence (SI) group (n = 24), RNS +blank virus (V) group (n = 6). Cutaneous sensitivity to thermal and mechanical stimulation was measured every two weeks after birth until 9 weeks of age (P7, P21, P35, P49, P63). Morris water maze (MWM) test was examined every 3 weeks after birth. RNS rats without pain/memory impairment-like behavior were not included in the analysis, and the number of each group which failed to demonstrate impairments was substituted by additional RNS rats. On week 9, all rats were killed and the hippocampus was harvested for further analyses. The individual doing behavioral testing of the rats was blinded to the treatment groups of animals.

Animal model of neonatal RNS

The neonatal RNS rat model was established as described (Anand et al., 1999) with some modifications. To model repetitive pain exposure in infants in the NICU, rat pups were stimulated with repetitive needle pricks on all four feet in succession every 6 h at 0:00, 6:00, 12:00 and 18:00 from the day of birth (P0) to P7. For this purpose, a 28G blood glucose needle was rapidly inserted into the middle plantar of rats' paw, and the control group received tactile stimulation with a cotton-tipped swab with identical stimulation place and time interval. At the end of each stimulation, the pups were put back to the original cage after sufficient hemostasis by cotton swab, ensuring that the time of mother-child separation was not more than 5 min in order to minimize the confounding long-term effect of mother-child separation on the experimental results. All rats were reared identically from P7 to P22, weaned on P23, and housed in sex-matched cages.

DNA constructs, cell culture, transfection, cell line establishment

Rat PRG-1 was amplified by One-Step RT-PCR Kit (Roche) using mRNA from rat cortex. PRG-1 coding sequence was cloned into pIRESneo3 (Clontech) between NheI and BamHI restriction sites to generate pIRESneo3-PRG-1; the R346T mutant of PRG-1 (PRG-1-R346T) was constructed using QuickChangeII XL Site-Directed Mutagenesis Kit (Stratagene).

HEK-293 cell lines were cultured in DMEM (Gibco) supplemented with 10% fetal bovine serum (PanBiotech), 100 U/mL penicillin, 100 μg/mL streptomycin, 2 mM L-glutamine and 0.1 mM MEM non-essential amino acids (all from Gibco) at 37°C/5% CO2. Stable cell lines were established by continual application of G418 (600 μg/mL) in complete DMEM after lipofectamine 2000 (invitrogen) transfection, and followed by picking and amplifying antibiotic resistant clones according to standard protocol.

METHOD DETAILS

Implantation of hippocampal cannula and microinjection procedures

After anesthesia with pentobarbital sodium (50 mg/kg body weight, intraperitoneal, i.p.), the rats were placed on a stereotaxic frame (RWD Life Science, China). The skull was exposed and the lentivirus

expression vector LV-Plppr4 or LV-Plppr4-RNAi (Genechem, Shanghai) was slowly injected (0.5 μL unilateral, 200 nL/min) bilaterally into the hippocampus area through a fine glass pipette via microsyringe pump (RWD Life Science, China) on P21. The pipette remained in place for 10 min to ensure complete diffusion of the virus and then slowly removed (Luo et al., 2018). The stereotaxic coordinates of hippocampus on P21 were AP = −3.10 mm, ML = ±1.7 mm, and DV = −2.5 mm, according to the rat brain atlas (Paxinos and Watson, 2007) with appropriate modification.

For drug, including ATP (Sigma, Germany), ATPγS (Sigma, Germany), treatment experiments, a guide cannula [0.48 mm outside diameter (O.D.); 0.34 mm inner diameter (I.D.)] was implanted into the hippocampus and fixed to the skull of rats on P53. For microinjection, rats were inserted with an injection cannula (0.3 mm O.D.; 0.5 mm longer than the guide cannula) into the guide cannula. A total volume of 0.5 μL drug solution was slowly injected, and the injector kept in place for 10 min to allow complete diffusion of the drug before slowly being withdrawn between P60-P62. Microinjection sites were checked by histological examination (Li et al., 2018). The stereotaxic coordinates of hippocampus were AP = −3.72 mm, ML = ±2.0 mm, and DV = −3.0 mm, according to the rat brain atlas (Paxinos and Watson, 2007).

Behavioral assessment

Inclined plane test

Motor function deficits including muscular strength and proprioception, were quantitated using an inclined plane as reported by Rivlin et al. (Rivlin and Tator, 1977). Rats at 9 weeks of age were placed crosswise on an inclined plane which can be adjusted to provide a slope of varying grade. The initial angle of the inclined plane was 25°, and the angle was increased slowly by 5°. The maximum angle of the plane at which the rats can maintain their position for 5 s without falling was recorded. The average values from the measurements of five times for each rat were defined as the inclined plane degree.

Radiant heat test

Thermal hyperalgesia was tested in rats as reported by Hargreaves et al. (1988) previously to evaluate thermal withdrawal latency (TWL). Each rat was placed in an individual Plexiglass house, allowed to acclimate for 30 min, then 52 ± 0.2°C radiant heat (50 W, 8 V bulb) was applied to the plantar surface of the hind paw with a plantar radiant heat instrument (IITC Life Science Instruments, USA). Latency period was recorded until the removal of the paw (including lifting, licking, flicking, shaking or jumping). The cut-off limit was set to 60 s. Each hind paw was measured five times at 5-min intervals (Liu et al., 2021b).

The electronic von Frey meter test for mechanical withdrawal threshold (MWT)

Mechanical allodynia of rat hind paw was used to evaluate MWT with the electronic von Frey anesthesiometer (IITC Life Science Instruments, USA), as described by Vivancos GG et al. (Vivancos et al., 2004). Each rat was placed in an individual plastic chamber for 30 min and allowed to acclimate. The polypropylene tip was applied to the plantar surface of the hind paw with a gradual increase in pressure until a functional response occurred (e.g., lifting, licking, flicking, shaking or jumping). The threshold pressure was recorded. Each hind paw was measured five times at 5-min intervals.

Morris water maze (MWM) test

Spatial learning and memory abilities were tested by the MWM hidden platform task as reported by previous studies (Vorhees and Williams, 2006; Wan et al., 2021). Briefly, 6 rats in each group were randomly selected for MWM test. The CON and RNS groups were tested at week 3 (P22–P26), week 6 (P43–P47) or week 9 (P64–P68), and the drug or virus injected groups were tested only at week 9 (P64–P68). A circular pool (a height of 50 cm and a diameter of 150 cm) was filled with tap water (22–24°C) to a depth of 30 cm. A hidden platform was positioned below the water at the center of the same quadrant for days 1–4. On four consecutive days, rats were released from quadrants I, II, III, and IV and performed four trials per day, and the starting positions were randomized for each rat. The rat found the platform with a maximal observation length of 90 s. The time it took was recorded as escape latency. If rats did not find the platform within 90 s, they were guided gently to the platform and allowed to stay on it for 10 s. On the fifth day, a probe trial (60 s) was performed without platform. The time that the rat stayed in the quadrant zone of the previous platform location within 60 s was recorded. Mean speed in MWM is also calculated to evaluate motor function. The path and duration in defined test compartments of each rat were automatically recorded with a computerized video Smart 3.0 system (Panlab, Spain).

Perfusion and immunofluorescence

Rats were deeply anesthetized with pentobarbital sodium (50 mg/kg body weight, i.p.) before the perfusion of normal saline (NS) through the left ventricle followed by 4% PFA. Brains were dissected, post-fixed in 4% PFA for 4–6 h at 4°C, and cryoprotected in 30% sucrose at 4°C until sank. The brains were then coronally sliced at a thickness of 30 μm on a cryostat (Leica CM 1950, Germany).

For immunofluorescence, the sections were blocked and permeabilized, and then incubated with rabbit anti-rat PRG-1 antibody (1:500, synaptic system). Sections were incubated in secondary donkey anti-rabbit antibody conjugated with CY3 (1:1000, Abcam). The captured images were observed under a fluorescence microscope (Olympus DP80, Japan).

Co-immunoprecipitation (CoIP) and western blot (WB)

The dissected and mechanically homogenized whole hippocampus or HEK-293 cells, were lysed in appropriate volume of RIPA lysis buffer (Beyotime, China) containing PMSF (YEASEN) for 1 h on ice, and cleared by centrifugation for 10 min at 15,000 g at 4°C. Protein concentrations of the lysate were determined using Bradford reagent (Bio-Rad, Hercules, CA, USA).

For co-immunoprecipitation, the lysate was first cleared with agarose slurry, incubated with PRG-1 antibody (1:100, synaptic system) or normal rabbit IgG (1:100, Millipore) as control, then pulled down by Protein G agarose resin (absin). Finally, beads were suspended with appropriate amount of lysis buffer and analyzed by western blot.

For western blot, tissue or cell lysates were separated by 10% SDS-PAGE and transferred onto PVDF membrane (Biosharp). Membranes were then incubated with first antibodies, including PRG-1 (1:3000, synaptic system), GluR2 (1:3000, Novus), NSF (1:3000, Abcam), β-actin (1:5000, MP Biomedicals), washed, and then incubated with horseradish peroxidase (HRPO)-conjugated secondary antibodies (1:5000, dianova). Finally, membranes were developed by enhanced chemiluminescence procedure (ECL, EpiZyme scientific). Quantification of immunosignals was performed using ImageJ.

Nissl staining

Nissl staining was used to identify nissl bodies in the neuronal cytoplasm. The frozen hippocampal sections were washed with distilled water after 4% PFA fixing for 20 min. Sections were then stained with nissl staining solution (Beyotime) for 3–10 min according to the dyeing results and requirements. Sections were washed twice with distilled water and then 70% ethanol. Finally, nissl bodies images were obtained using a microscope (Olympus DP80, Japan) (Huang et al., 2020).

Golgi-Cox staining and dendritic synapse quantification

Golgi staining was used to examine neuroplasticity. After anesthesia, rat brains were removed and immediately stained by Hito Golgi-Cox OptimStain^{TM} Kit (Hitobiotec, USA) according to the manufacturer's instructions and then photographed under a microscope (Olympus DP80, Japan). Spines were defined as dendritic protrusions and were manually counted along a selected dendritic segment using Image J 6.0 software (NIH, USA) (Theer et al., 2014; Zhao et al., 2020). In brain sections, the three areas of dendrites examined were: (1) the middle molecular layer of dentate gyri (moDG) granule cells; (2) stratum radiatum (sr, apical dendrites) and (3) stratum oriens (so, basal dendrites) of pyramidal neurons of the CA1 region. For each group around 1000 spines or at least 1000 μm dendritic length were measured. Additionally, the dendritic spine density, that is, the number of spines per μm dendrite was calculated (Liu et al., 2016). Analysis was performed by researchers blinded to the treatment group.

Enzyme-linked immunosorbent assay (ELISA) of glutamate

Hippocampal tissues in each group were homogenized in PBS buffer containing PMSF (YEASEN) at a general weight/volume (mg/μL) ratio of 1:9 using a homogenizer on ice. The homogenates were centrifuged at 5,000 g for 10 min at 4°C, and the supernatant was collected to represent extracellular protein. Glutamate was detected following protocol of rat glutamic acid (Glu) ELISA Kit (Jianglai, China). The concentration of glutamate was calculated according to the curve equation.

RNA extraction and quantitative reverse transcription polymerase chain reaction (qRT-PCR)

RNA was extracted from hippocampal tissue using TRIzol and reverse-transcribed into cDNA using the PrimeScript™ RT reagent Kit (Takara, Japan). Differential target gene expression was analyzed following polymerase chain reaction (PCR) using the TB Green® Premix Ex Taq™ II (Takara). The relative expression was defined as $F = 2^{-\Delta\Delta ct}$. Primers were synthesized by Sangon (Shanghai, China) and listed in Table S2.

QUANTIFICATION AND STATISTICAL ANALYSIS

Data were processed using GraphPad Prism (version 8.0.2; GraphPad Software, Inc., USA). Results are expressed as the mean ± SEM (standard error of mean) if not otherwise indicated. Normal distribution was assessed using the Kolmogorov-Smirnov-Test. Statistical analysis was performed using two-tailed unpaired student t-test for comparing two groups with normally distributed data or a Mann-Whitney-U test for comparing two groups containing nonparametric distributed data. Data normalized to control values (rendering control values as 1) were calculated using a one-sample t test with normal distributed data or Wilcoxon signed-rank test for comparing groups containing nonparametric distributed data. One-way analysis of variance (ANOVA) with Bonferroni correction was used for comparing multiple groups containing normally distributed data or a Kruskal-Wallis test with a Dunn's multiple comparisons test for comparing multiple groups containing nonparametric distributed data. For comparison of multiple groups containing two factors, a two-way ANOVA with repeated measures followed by Tukey's post-hoc multiple comparisons test was used. Statistical significance was determined with an overall significance level of $p < 0.05$ (n.s. for $p > 0.05$, *$p < 0.05$, **$p < 0.01$, ***$p < 0.001$).